Inorganic Chemistry

ARTICLE

pubs.acs.org/IC

A Unique Dinuclear Mixed V(V) Oxo-peroxo Complex in the Structural Speciation of the Ternary V(V)-Peroxo-citrate System. Potential Mechanistic and Structural Insight into the Aqueous Synthetic Chemistry of Dinuclear V(V)-Citrate Species with H_2O_2

M. Kaliva,[†] C. Gabriel,[‡] C. P. Raptopoulou,[§] A. Terzis,[§] G. Voyiatzis,[▽] M. Zervou,[⊥] C. Mateescu,[○] and A. Salifoglou*[,‡]

[†]Department of Chemistry, University of Crete, Heraklion 71409, Greece

[‡]Laboratory of Inorganic Chemistry, Department of Chemical Engineering, Aristotle University of Thessaloniki, Thessaloniki 54124, Greece

[§]Institute of Materials Science, NCSR "Demokritos", Aghia Paraskevi 15310, Attiki, Greece

[▽]Foundation for Research and Technology Hellas (FORTH), Institute of Chemical Engineering and High Temperature Chemical Processes (ICE/HT), Patras 26500, Greece

[⊥]Laboratory of Molecular Analysis, Institute of Organic and Pharmaceutical Chemistry, National Hellenic Research Foundation, Athens 11635, Greece

[○]Banat University of Agricultural Sciences and Veterinary Medicine, Timisoara 1900, Romania

Supporting Information

ABSTRACT: Diverse vanadium biological activities entail complex interactions with physiological target ligands in aqueous media and constitute the crux of the undertaken investigation at the synthetic level. Facile aqueous redox reactions, as well as nonredox reactions, of V(III) and V(V) with physiological citric acid and hydrogen peroxide, under pH-specific conditions, led to the synthesis and isolation of a well-formed crystalline material upon the addition of ethanol as the precipitating solvent. Elemental analysis pointed to the molecular formulation $(NH_4)_4[(VO_2)\{VO(O_2)\}(C_6H_5O_7)_2]\cdot 1.5H_2O$ (**1**). Complex **1** was further characterized by Fourier transform infrared (FT-IR) spectroscopy, nuclear magnetic resonance (NMR), Raman spectroscopy, cyclic voltammetry, and X-ray crystallography. The crystallographic structure of **1** reveals the presence of the first dinuclear V(V)-citrate complex with non-peroxo- and peroxo-containing V(V) ions, concurrently present within the basic $V^V_2O_2$ core. The nonperoxo unit VO_2^+ and the peroxo unit $VO(O_2)^+$ are each coordinated to a triply deprotonated citrate ligand in a distinct coordination mode and coordination geometry around the V(V) ions. These units are similar to those in homodinuclear complexes bearing oxo or peroxo groups. The unique assembly of both units in the anion of **1** renders the latter as a potential intermediate in the peroxidation process, from $[V_2O_4(C_6H_5O_7)_2]^{4-}$ to $[V_2O_2(O_2)_2(C_6H_6O_7)_2]^{2-}$. The transformation reactions of **1** establish its connection with several V(V) and V(IV) dinuclear species present in the aqueous distribution of the V(IV,V)-citrate systems. The shown position of **1** as an intermediate in the mechanism of H_2O_2 addition to dinuclear V(V)-citrate species portends its role in the complex aqueous distribution of species in the ternary V(V)-peroxo-citrate system and its potential reactivity in (bio)chemically relevant media.

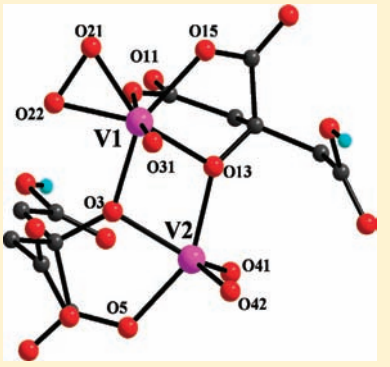

INTRODUCTION

A diverse spectrum of activities has been established over the years for vanadium in biological as well as abiotic systems.[1] In nature,[2] the presence of vanadium as an inorganic co-factor and catalytic center has been shown to cover many enzymes with key roles in haloperoxidation,[3] nitrogen fixation,[4,5] and elsewhere. Equally important is the involvement of vanadium in the physiology of organisms, affecting biological pathways, promoting antitumorigenicity,[6] mitogenicity,[7] and inhibition of key metabolic enzymes such as phosphoglucomutases and others.[8] Outstanding, however, among the various physiological activities of vanadium is the pharmacological efficacy of its biologically relevant ionic form(s) to act as an insulin mimetic agent, ameliorating the symptoms of the heterogeneous syndrome of diabetes mellitus.[9−11]

To the degree that vanadium gets involved in complex interactions with physiological ligands in biological media, its two predominant oxidation states, V(IV) and V(V), are key to influencing the associated chemistry and potentially ensuing

Received: June 5, 2011
Published: October 26, 2011

biological activity. Among the physiological ligands that could interact with vanadium are (a) the α-hydroxycarboxylic acid citric acid and (b) hydrogen peroxide. Both of these ligands belong to the class of low-molecular-mass targets and may constitute the first line of interaction upon which further ternary chemistries with both low- and high-molecular-mass targets unfold in the presence of vanadium. Citric acid is fairly abundant in biological fluids,[12] participating in the Krebs cycle and potentiating solubilization of metal ions through complexation. Solubility is the prerequisite for the bioavailability of a species emerging into the biological arena. Hydrogen peroxide, on the other hand, has been known for its redox properties and its potential binding ability to several metal ions, including vanadium.

Ternary interactions of vanadium with the two aforementioned ligands involve intricate speciation schemes, encompassing various species, as a function of the concentration and pH. In view of the fact that bioavailability emerges from speciation distributions in aqueous media, it is crucial that relevant information is available in order to seek and assess the potential activities and role(s) of vanadium in biological media. To this end, solution speciation studies are extremely important; yet, as such, they are very scarce in the case of the ternary V(V)-H_2O_2-citrate system.[13] Support of such studies comes from synthetically isolated ternary V(V)-H_2O_2-citrate dinuclear species containing both V(V) ions bound to peroxide moieties.[14−17] Numerous studies, on the other hand, exist on binary systems of V(IV) and V(V) (denoted hereafter as V(IV,V)) with citric acid and other biologically relevant ligands in aqueous media.[18,19] On an equal footing to ternary species, structurally characterized synthetic nonperoxo V(IV,V)-citrate complexes formulate a well-defined picture of the binary vanadium-citrate aqueous speciation.[20−23] In all of the aforementioned investigated systems (binary and ternary), structurally characterized dinuclear complexes exemplify the pH dependence of the vanadium chemical reactivity at different oxidation states and reflect the full complement of nonperoxo as well as peroxo vanadium-hydroxycarboxylate moieties in V_2O_2-containing core units. However, no mixed nonperoxo/peroxo vanadium-hydroxycarboxylate dinuclear species exist to date, reflecting (a) the importance of such complexes in the aqueous speciation and (b) the physicochemical properties of concurrent nonperoxo and peroxo moieties in a dinuclear vanadium unit that influence its chemical reactivity.

In view of the available information on the above-mentioned ternary system, research efforts were undertaken to pursue the synthesis and isolation of unique ternary V(V)-peroxo-citrate species in aqueous media, under specific pH conditions. To this end, facile aqueous redox as well as nonredox reactions of V(III) and V(V) (denoted hereafter as V(III,V)) with physiological citric acid and hydrogen peroxide, under pH-specific conditions, were investigated and led to a unique dinuclear species. Hence, herein, we report the synthesis, isolation, and spectroscopic and structural characterization of a unique V(V)-peroxo-citrate complex, displaying a mixed nonperoxo and peroxo vanadium basic $V^V_2O_2$ core. The importance of such a species reflects a potential pathway for hydrogen peroxide addition on known $V^V_2O_2$ core dinuclear complexes in aqueous media. The possible implications of such chemistry, and its associated biological ramifications, are also discussed in the context of the aqueous chemistry and speciation of vanadium with citrate and peroxide.

EXPERIMENTAL SECTION

Materials and Methods. All experiments were carried out under aerobic conditions. Nanopure-quality water was used for all reactions. VCl_3, V_2O_5, anhydrous citric acid, and H_2O_2 30% were purchased from Aldrich. Ammonia was supplied by Fluka.

Physical Measurements. Fourier transform infrared (FT-IR) spectra were recorded on a Model 1760X FT-infrared spectrometer (Perkin−Elmer). Ultraviolet−visible light (UV-Vis) measurements were carried out on a Model U2001 spectrophotometer (Hitachi) in the wavelength range from 190 nm to 1000 nm. A Model Flash EA 1112 CHNS elemental analyzer (ThermoFinnigan) was used for the simultaneous determination of carbon, hydrogen, and nitrogen content (expressed as a percentage). The analyzer is based on the dynamic flash combustion of the sample (at 1800 °C), followed by reduction, trapping, complete GC separation, and detection of the products. The instrument is (a) fully automated and is controlled by PC via the Eager 300 dedicated software, and (b) capable of handling solid, liquid, or gaseous substances.

Solid-State NMR Spectroscopy. Solid state cross-polarized magic angle spinning (CP-MAS) ^{13}C NMR spectra were obtained on a Model MSL400 NMR spectrometer (Bruker). The high-resolution solid-state CP-MAS ^{13}C NMR spectra were measured at 100.61 MHz. The spinning rate used was 10.0 kHz at 0 °C. The solid-state spectrum was a result of the accumulation of 1024 scans. The recycle delay used was 2 s, the 90° pulse was 2.4 μs, and the contact time was 1 ms. All solid-state spectra were referenced to adamantane, which showed two peaks at 26.5 and 37.6 ppm, respectively, and to the external reference of trimethylsilane (TMS).

MAS ^{51}V NMR spectra were measured at a frequency of 105.25 MHz (magnetic field = 9.4 T) and a spinning rate of 11.77 kHz at 0 °C. Different spinning speeds were employed and comparative measurements under a magnetic field of 17.6 T (frequency = 197.07 MHz) were taken in order to identify isotropic peaks as those signals that do not change their shift value with varying measurement parameters. For the presented spectrum, 128 accumulations with a recycle delay of 1.5 s and a 90° pulse length of 0.3 μs were obtained. The spectral window was set to 1 MHz, and referencing was done with a 0.16 M solution of $NaVO_3$ as a secondary reference at −574 ppm, with respect to $VOCl_3$.[24]

Solution NMR Spectroscopy. Solution ^{13}C NMR experiments for complex **1** were carried out on a Varian 600 MHz spectrometer. The sample concentration was ∼0.02−0.10 M. The compound was dissolved in D_2O. The ^{13}C spectral width was 30 000 Hz. Experimental data were processed using V NMR routines. Spectra were zero-filled twice and apodized with a squared sinusoidal bell function shifted by π/2 in both dimensions. Chemical shifts (δ) of ^{13}C resonance peaks are reported in units of ppm, relative to the adamantane ($C_{10}H_{16}$) CH group that was used as an external reference.

Fourier Transform−Raman (FT-Raman) Spectroscopy. Fourier transform−Raman (FT-Raman) measurements were obtained using a Bruker (D) FRA-106/S component attached to an EQUINOX 55 spectrometer. A R510 diode-pumped Nd:YAG polarized laser at 1064 nm (with a maximum output power of 500 mW) was used for Raman excitation in a 180° scattering sample illumination mode. Optical filtration reduced the Rayleigh elastic scattering and, in combination with a CaF_2 beam splitter, as well as a high-sensitivity liquid-nitrogen-cooled germanium detector, allowed Raman intensities to be recorded from 50 cm^{-1} to 3300 cm^{-1} in the Stokes-shifted Raman region, all in one spectrum. The resulting spectra were an average of 300 scans, recorded at a resolution of 2 cm^{-1}; the laser was focused onto the sample on a circular area ∼100 μm in diameter, with an output power of ∼100 mW. Similar results were obtained utilizing 100 scans recorded at a resolution of 4 cm^{-1} with an output laser power of 300 mW on the sample. The spectra were corrected for scattering, since Rayleigh's ν^4-law relates the scattering as a function of the wavenumber. The FT-Raman calibration test that utilized cyclohexane gave a peak frequency uncertainty of ±0.95 cm^{-1} at ∼1000 cm^{-1}.

Electrochemical Measurements. Electrochemical measurements were carried out with a Model PG580 potentiostat−galvanostat (Uniscan Instruments, Ltd.). The entire system was under computer

control and supported by the appropriate computer software Ui Chem Version 1.08RD, running on Windows. The electrochemical cell used had platinum (disk) working and auxiliary (wire) electrodes. As a reference electrode, a Ag/AgCl electrode was used. The water used in the electrochemical measurements was of nanopure quality. Potassium nitrate (KNO_3) was used as a supporting electrolyte. Normal solution concentrations used were 1−6 mM in electroanalyte and 0.1 M in the supporting electrolyte. Purified argon was used to purge the solutions prior to the electrochemical measurements.

Preparation of Complexes. *(a). $(NH_4)_4[(VO_2)\{VO(O_2)\}(C_6H_5O_7)_2]\cdot 1.5H_2O$ (**1**). Method 1.* A sample of V_2O_5 (0.20 g, 1.1 mmol) was dissolved in 3 mL of H_2O, and a solution of ammonia (0.30 mL of a 1:1 aqueous solution) was added slowly under stirring. The derived mixture was subjected to stirring overnight at 50 °C. On the following day, the reaction mixture had turned into a milky emulsion. To that, a quantity of anhydrous citric acid (0.80 g, 4.2 mmol) was added under stirring. The resulting reaction mixture became orange in color and clear and remained as such. The pH of the solution was then adjusted with aqueous ammonia to pH 4.5. Subsequently, the reaction mixture was placed in an ice bath and a 30% solution of hydrogen peroxide (1.8 mL, 18 mmol) was slowly added to it and under continuous stirring. Stirring continued for an additional 10 min in ice without any change in the color of the solution. The reaction mixture then was placed in the refrigerator (4 °C). The next morning, the solution was red and cold ethanol was added periodically until a red crystalline material had precipitated. The product was isolated by filtration and dried in vacuo. Yield: 0.30 g (55%). Anal. Calcd. for **1**, $(NH_4)_4[(VO_2)\{VO(O_2)\}(C_6H_5O_7)_2]\cdot 1.5H_2O$ ($C_{12}H_{29}N_4O_{20.5}V_2$, MW = 659.27): C, 21.84; H, 4.39; N, 8.49. Found: C, 21.76; H, 4.42; N, 8.44.

Method 2. An amount of VCl_3 (0.13 g, 0.80 mmol) and anhydrous citric acid (0.15 g, 0.78 mmol) were dissolved in 3 mL of water. The pH of the resulting solution was adjusted to ∼8.5 with aqueous ammonia. The solution was initially green. Following overnight stirring at room temperature, the color of the solution turned blue and the pH was 7.7. The reaction flask then was placed in an ice bath, and a 30% H_2O_2 solution (0.72 mL, 7.0 mmol) was added dropwise and under continuous stirring. The color of the solution turned orange, and stirring continued for an additional 20 min on ice. The reaction mixture then was placed in the refrigerator (4 °C). On the following day, the solution was red and cold ethanol was added periodically until red crystals formed at the bottom of the flask. The crystalline product was isolated by filtration and dried in vacuo. Yield: 0.085 g (32%). Positive identification of the crystalline material as complex **1** came from the FT-IR spectrum and the X-ray unit-cell determination that was carried out on a single crystal.

*(b). Interconversions. From $(NH_4)_4[(VO_2)\{VO(O_2)\}(C_6H_5O_7)_2]\cdot 1.5H_2O$ (**1**) to $(NH_4)_4[V_2O_2(C_6H_4O_7)_2]\cdot 2H_2O$ (**2**).*[21] A quantity of the complex $(NH_4)_4[(VO_2)\{VO(O_2)\}(C_6H_5O_7)_2]\cdot 1.5H_2O$ (0.080 g, 0.12 mmol) was placed in a 25-mL round-bottom flask and dissolved in 3 mL of water. The color of the resulting solution was red, and the pH was ∼4.5. The solution was subjected to stirring at 50 °C overnight. The following day, the pH was 6.5 and the color of the solution was blue and did not change any further. The pH of the solution was adjusted with aqueous ammonia (1:1 ammonia:water) to ∼8. After brief stirring at room temperature, the solution was taken to dryness by means of a rotary evaporator. The residue was redissolved in a minimum volume of a warm mixture of isopropanol and water−ethanol. Subsequently, the reaction flask was stored at 4 °C. A few days later, blue crystals appeared at the bottom and on the sides of the flask. The crystals were isolated by filtration and dried in vacuo. The yield was 0.035 g (29%). The FT-IR of the crystalline material was identical to that of an authentic sample of $(NH_4)_4[V_2O_2(C_6H_4O_7)_2]\cdot 2H_2O$.

*From $(NH_4)_4[(VO_2)\{VO(O_2)\}(C_6H_5O_7)_2]\cdot 1.5H_2O$ (**1**) to $(NH_4)_4[V_2O_4(C_6H_5O_7)_2]\cdot 4H_2O$ (**3**).*[28] A quantity of $(NH_4)_4[(VO_2)\{VO(O_2)(C_6H_5O_7)_2]\cdot 1.5H_2O$ (0.15 g, 0.23 mmol) was placed in a 25-mL round-bottom flask and dissolved in 3.0 mL of water. The color of the resulting solution was red, and the pH ∼4.5. The solution was subjected to stirring for 1 h at 50 °C. During that period of time, the color of the reaction solution turned yellow and remained as such. Following brief stirring at room temperature, ethanol was added and the reaction flask was stored at 4 °C. A few days later, yellowish crystals appeared at the bottom of the flask. These crystals were isolated by filtration and dried in vacuo. The yield of the transformation was 0.028 g (18%). The FT-IR spectrum of the crystalline material revealed that the product of the transformation was $(NH_4)_4[V_2O_4(C_6H_5O_7)_2]\cdot 4H_2O$.

*From $(NH_4)_4[V_2O_4(C_6H_5O_7)_2]\cdot 4H_2O$ (**3**) to $(NH_4)_4[(VO_2)\{VO(O_2)\}(C_6H_5O_7)_2]\cdot 1.5H_2O$ (**1**).* A quantity of $(NH_4)_4[V_2O_4(C_6H_5O_7)_2]\cdot 4H_2O$ (0.35 g, 0.52 mmol) was placed in a 25-mL round-bottom flask and dissolved in 3.0 mL of water. The resulting solution was orangish in color, and the pH was ∼4.5. The solution was placed in an ice bath and a 30% H_2O_2 solution (0.83 mL, 8.2 mmol) was added slowly and under continuous stirring. At the end, the resulting solution was further stirred in ice for 10 min. During that period of time, the color of the reaction solution turned orange and remained as such. The reaction flask then was placed in a refrigerator (4 °C). The next day, the color of the solution was red. Absolute ethanol was added and, a few days later, red crystals appeared at the bottom of the flask; these crystals were isolated by filtration and dried in vacuo. The yield of the transformation was 0.070 g (21%). The FT-IR spectrum of the crystalline material revealed that the product of the transformation was $(NH_4)_4[(VO_2)\{VO(O_2)\}(C_6H_5O_7)_2]\cdot 1.5H_2O$.

*From $(NH_4)_4[V_2O_4(C_6H_5O_7)_2]\cdot 4H_2O$ (**3**) to $(NH_4)_2[V_2O_2(O_2)_2(C_6H_6O_7)_2]\cdot 2H_2O$ (**5**).* A quantity of $(NH_4)_4[V_2O_4(C_6H_5O_7)_2]\cdot 4H_2O$ (0.47 g, 0.68 mmol) was placed in a 25-mL round-bottom flask and dissolved in 3.0 mL of water. The color of the resulting solution was orangish, and the pH was ∼4.5. The pH of the solution was adjusted with dilute hydrochloric acid (HCl) to ∼3.5. The solution was placed in an ice bath and a 30% H_2O_2 solution (1.12 mL, 11.0 mmol) was added slowly and under continuous stirring. At the end, the resulting solution was further stirred on ice for 10 min. During that period of time, the color of the reaction solution turned orange and remained as such. The reaction flask then was placed in a refrigerator (4 °C). The next day, the color of the solution was red. Absolute ethanol was added and, a few days later, red crystals appeared at the bottom of the flask; these crystals were isolated by filtration and dried in vacuo. The yield of the transformation was 0.070 g (17%). The FT-IR spectrum of the crystalline material revealed that the product of the transformation was $(NH_4)_2[V_2O_2(O_2)_2(C_6H_6O_7)_2]\cdot 2H_2O$.

*From $(NH_4)_4[(VO_2)\{VO(O_2)\}(C_6H_5O_7)_2]\cdot 1.5H_2O$ (**1**) to $(NH_4)_2[V_2O_4(C_6H_6O_7)_2]\cdot 2H_2O$ (**4**).* A quantity of $(NH_4)_4[(VO_2)\{VO(O_2)\}(C_6H_5O_7)_2]\cdot 1.5H_2O$ (0.30 g, 0.45 mmol) was placed in a 25-mL round-bottom flask and dissolved in 3.0 mL of water. The color of the resulting solution was red, and the pH was ∼4.2. The solution was subjected to stirring for 4 h at room temperature. During that period of time, the color of the reaction solution turned orange and remained as such. The pH of the resulting reaction solution was 4.2. Subsequently, ethanol was added and the reaction flask was stored at 4 °C. A few days later, yellowish crystals appeared at the bottom of the flask, which were isolated by filtration and dried in vacuo. The yield of the transformation was 0.10 g (36%). The FT-IR spectrum of the crystalline material revealed that the product of the transformation was $(NH_4)_2[V_2O_4(C_6H_6O_7)_2]\cdot 2H_2O$.

*From $(NH_4)_4[(VO_2)\{VO(O_2)\}(C_6H_5O_7)_2]\cdot 1.5H_2O$ (**1**) to $(NH_4)_2[V_2O_2(O_2)_2(C_6H_6O_7)_2]\cdot 2H_2O$ (**5**).* A quantity of $(NH_4)_4[(VO_2)\{VO(O_2)\}(C_6H_5O_7)_2]\cdot 1.5H_2O$ (0.15 g, 0.23 mmol) was placed in a 25-mL round-bottom flask and dissolved in 3.0 mL of water. The color of the resulting solution was red, and the pH was ∼4.5−5.0. The pH of the solution was adjusted to ∼4.0 with dilute HCl. The reaction flask was placed in an ice bath and a 30% H_2O_2 solution (0.15 g, 4.5 mmol) was added slowly and under continuous stirring. At the end, the resulting solution was stirred in ice for an additional 10 min. During that period of time, the color of the reaction solution turned red and the pH was ∼4. Subsequently, ethanol was added and the reaction flask was stored at 4 °C. A few days later, orange-red crystals

Table 1. Summary of Crystal, Intensity Collection, and Refinement Data for $(NH_4)_4[(VO_2)\{VO(O_2)\}(C_6H_5O_7)_2]\cdot 1.5H_2O$ (1)

parameter	value
formula	$C_{12}H_{29}N_4O_{20.5}V_2$
formula weight, FW	659.27
temperature, T (K)	298
wavelength (nm)	Mo Kα, 0.71073
space group	$I2/a$
unit-cell parameters	
a (Å)	20.833(8)
b (Å)	9.235(4)
c (Å)	25.68(1)
β (deg)	95.19(1)
volume, V (Å^3)	4920(4)
Z	8
D_{calcd} (Mg m^{-3})	1.780
D_{measd} (Mg m^{-3})	1.79
abs. coeff., μ (mm^{-1})	0.862
range of h, k, l	−24→24, −10→0, 0→30
goodness-of-fit (GOF) on F^2	1.059
R^a	R = 0.0417^b
$R_w{}^a$	R_w = 0.1069^b

[a] R values are based on F values; R_w values are based on F^2 values: $R = \Sigma(||F_o| - |F_c||)/\Sigma|F_o|$, $R_w = \{\Sigma[w(F_o^2 - F_c^2)^2]/\Sigma[w(F_o^2)^2]\}^{1/2}$. [b] For 3783 reflections with $I > 2\sigma(I)$.

appeared at the bottom of the flask. These crystals were isolated by filtration and dried in vacuo. The yield of the transformation was 0.035 g (24%). The FT-IR spectrum of the crystalline material revealed that the product of the transformation was $(NH_4)_2[V_2O_2(O_2)_2(C_6H_6O_7)_2]\cdot 2H_2O$.

*From $(NH_4)_6[V_2O_4(C_6H_4O_7)_2]\cdot 6H_2O$ (**6**) to $(NH_4)_4[(VO_2)\{VO(O_2)\}(C_6H_5O_7)_2]\cdot 1.5H_2O$ (**1**).* A quantity of $(NH_4)_6[V_2O_4(C_6H_4O_7)_2]\cdot 6H_2O$ (0.32 g, 0.42 mmol) was placed in a 25-mL round-bottom flask and dissolved in 3.0 mL of water. The color of the resulting solution was orangish, and the pH was ∼7. The pH was adjusted with dilute HCl to ∼4.5. The solution then was placed in an ice bath and a 30% H_2O_2 solution (0.68 mL, 6.8 mmol) was added slowly and under continuous stirring. At the end, the resulting solution was stirred in ice for an additional 10 min. During that period of time, the color of the reaction solution turned orange and remained as such. Subsequently, the reaction flask was placed in the refrigerator (4 °C). The following day, the color of the solution had turned red. Ethanol was added and, a few days later, red crystals appeared at the bottom of the flask. These crystals were isolated by filtration and dried in vacuo. The yield of the transformation was 0.050 g (18%). The FT-IR spectrum of the crystalline material revealed that the product of the transformation was $(NH_4)_4[(VO_2)\{VO(O_2)\}(C_6H_5O_7)_2]\cdot 1.5H_2O$.

X-ray Crystallography. *Crystal Structure Determination.* X-ray-quality crystals of compound **1** were grown from water−ethanol mixtures. A single crystal, with dimensions of 0.60 mm × 0.22 mm × 0.45 mm (**1**), was mounted on a Crystal Logic dual-goniometer diffractometer, using graphite monochromated Mo Kα radiation. Unit-cell dimensions for **1** were determined and refined using the angular settings of 25 automatically centered reflections in the range of 11° < 2θ < 23°. Relevant crystallographic details are given in Table 1. Intensity data were measured using $\theta-2\theta$ scans. Three standard reflections were monitored every 97 reflections, throughout data collection, and showed <3% variation and no decay. Lorentz and polarization corrections were applied using Crystal Logic software. Further experimental crystallographic details for **1** are given as follows: $2\theta_{max}$ = 50°; reflections collected/unique/used, 4443/4331 (R_{int} = 0.0117)/4331; 443 parameters refined; $(\Delta\rho)_{max}/(\Delta\rho)_{min}$ = 0.830/−0.396 e/Å^3; Δ/σ = 0.004; goodness-of-fit (GOF) on F^2 = 1.059; R/R_w (for all data), 0.0489/0.1155.

The structure of complex **1** was solved by direct methods using SHELXS-97,[25] and refined by full-matrix least-squares techniques on F^2 with SHELXL-97.[26] All non-hydrogen atoms in **1** were refined anisotropically. All the H atoms were located by difference maps and were refined isotropically; no H atoms for the water solvate molecules were included in the refinement.

RESULTS

Syntheses. The complex $(NH_4)_4[(VO_2)\{VO(O_2)\}(C_6H_5O_7)_2]\cdot 1.5H_2O$ (**1**) was synthesized from simple reagents in aqueous solutions. Specifically, V_2O_5 was reacted with citric acid in the presence of ammonia. The role of aqueous ammonia was 2-fold. It was used to adjust the pH of the reaction medium at which the synthesis was carried out and, at the same time, provided the counterions necessary for balancing the negative charge on the derived anionic complex **1**.

The overall stoichiometric reaction leading to complex **1** is shown schematically below:

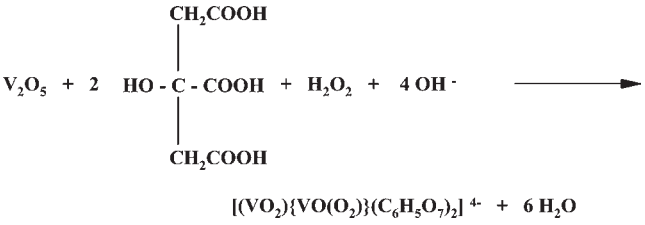

A redox reaction was also used, with VCl_3 and citric acid reacting in the presence of H_2O_2. The reactions were similar to those used for the synthesis of $K_4[V_2O_2(C_6H_5O_7)_2]\cdot 5.6H_2O$.[27] Initially, VCl_3 and citric acid reacted in water, in the presence of ammonia, and led to a blue solution.[21] Past synthetic studies on the specific chemistry had revealed that the blue species arising in the course of the reaction was a dinuclear V(IV)−citrate species, which was spectroscopically and structurally characterized.[21] A H_2O_2 solution was then added to the reaction mixture, finally giving a red crystalline material, the composition of which was consistent with the molecular formulation of **1**. The stoichiometric depiction of the reaction is shown below:

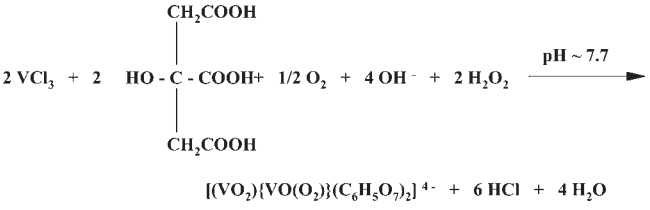

In both routes of the synthesis of complex **1**, precipitation of the product in a crystalline form, from the reaction mixture, was effected by adding ethanol at 4 °C. Elemental analysis on the NH_4^+ salt of the isolated crystalline materials suggested the formulation $(NH_4)_4[(VO_2)\{VO(O_2)\}(C_6H_5O_7)_2]\cdot 1.5H_2O$ for **1**. Positive identification of the crystalline product was achieved by FT-IR spectroscopy and X-ray crystallography for one of the isolated single crystals from **1**. Complex **1** is stable, in the crystalline form, in air for long periods of time (∼2−3 weeks). It is insoluble in alcohols (CH_3OH, *i*-PrOH), acetonitrile, and dimethyl sulfoxide (DMSO) at room temperature. It readily dissolves in water.

Interconversions. Initially, nonthermal transformations were attempted. Specifically, simple dissolution of complex $(NH_4)_4[(VO_2)\{VO(O_2)\}(C_6H_5O_7)_2]\cdot 1.5H_2O$ (**1**) in water and stirring for 3 h led to the isolation of complex $(NH_4)_2[V_2O_4(C_6H_6O_7)_2]\cdot 2H_2O$ (**4**) upon the addition of ethanol at 4 °C. A stoichiometric rendition of this reaction is shown in reaction 1:

$$[(VO_2)\{VO(O_2)\}(C_6H_5O_7)_2]^{4-}(\mathbf{1}) + 2H^+ + H_2O \rightarrow [V_2O_4(C_6H_6O_7)_2]^{2-}(\mathbf{4}) + H_2O_2 \quad (1)$$

This simple conversion revealed the facile departure of the peroxide group from the assembly of the anion in **1**, even at room temperature, thus denoting the limited stability of the peroxo complex in aqueous solutions. The $(NH_4)_2[V_2O_4(C_6H_6O_7)_2]\cdot 2H_2O$ complex had been synthesized, isolated, and spectroscopically and structurally characterized previously.[15]

In an extended heat treatment of an aqueous solution of **1** overnight, the color of the solution turned blue and remained as such. Adjustment of the pH to ~8 with ammonia ultimately led to the isolation of complex $(NH_4)_4[V_2O_2(C_6H_4O_7)_2]\cdot 2H_2O$ (**2**) in the presence of isopropanol (reaction 2).[21]

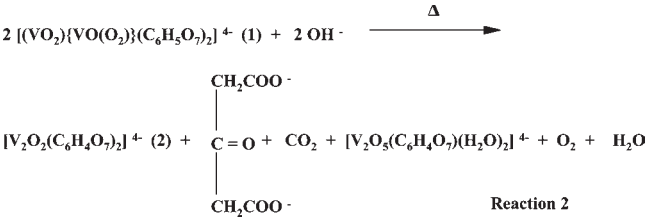

Reaction 2

It should be mentioned that the oxidation state of vanadium in complex **1** is +5, while the oxidation state of vanadium in $(NH_4)_4[V_2O_2(C_6H_4O_7)_2]\cdot 2H_2O$ is +4. Thus, under the conditions examined, there was a one-electron reduction per V(V) ion taking place, finally yielding the $V^{IV}{}_2O_2$ core-containing stable dinuclear complex (vide supra).[21]

In an analogous fashion, solutions of **1** were heat-treated under mild conditions (50 °C) for a shorter period of time (1 h). As a result, the addition of the precipitating solvent led to the isolation of complex $(NH_4)_4[V_2O_4(C_6H_5O_7)_2]\cdot 4H_2O$ (**3**). The stoichiometric reaction is given in reaction 3. The latter complex had been previously synthesized, isolated, and characterized crystallographically.[28]

$$[(VO_2)\{VO(O_2)\}(C_6H_5O_7)_2]^{4-}(\mathbf{1}) + H_2O \xrightarrow{\Delta} [V_2O_4(C_6H_5O_7)_2]^{4-}(\mathbf{3}) + H_2O_2 \quad (3)$$

The reverse reaction of adding H_2O_2 to complex **3** was promoted on a facile basis and led to the isolation and crystallization of complex **1**. The stoichiometric depiction of the reaction is shown as reaction 4:

$$[V_2O_4(C_6H_5O_7)_2]^{4-}(\mathbf{3}) + H_2O_2 \rightarrow [(VO_2)\{VO(O_2)\}(C_6H_5O_7)_2]^{4-}(\mathbf{1}) + H_2O \quad (4)$$

Thus, two things were shown: (a) there is a reversible conversion and connection between complex **1** and complex **3**, and (b) one peroxide group can be added upon the addition of H_2O_2 to complex **3**. The latter observation leads to the contention that **1** may be a suitable intermediate of the peroxidation of complex **3** and further generation of complex **5**.

Connectivity of complex **3** with complex **5** was also shown through reaction of the former species with H_2O_2. The stoichiometric reaction is shown in reaction 5:

$$[V_2O_4(C_6H_5O_7)_2]^{4-}(\mathbf{3}) + 2H_2O_2 + 2H^+ \rightarrow [V_2O_2(O_2)_2(C_6H_6O_7)_2]^{2-}(\mathbf{5}) + 2H_2O \quad (5)$$

The reaction establishes a direct link between the two complexes, thus lending support to **1** as a potential intermediate. A reverse conversion between the two species had been previously shown to exist for the K^+ salt of the two anionic complexes.[16]

Further exploration of the chemical reactivity of complex **1** included the addition of H_2O_2. In a straightforward reaction, excess H_2O_2 was added to achieve peroxidation of the only available nonperoxo vanadium site on complex **1**. As a result, the fully peroxidized dinuclear complex $(NH_4)_2[V_2O_2(O_2)_2(C_6H_6O_7)_2]\cdot 2H_2O$ (**5**) formed and was isolated.[15] The stoichiometric reaction is depicted as reaction 6:

$$[(VO_2)\{VO(O_2)\}(C_6H_5O_7)_2]^{4-}(\mathbf{1}) + H_2O_2 + 2H^+ \rightarrow [V_2O_2(O_2)_2(C_6H_6O_7)_2]^{2-}(\mathbf{5}) + H_2O \quad (6)$$

Acidification of the reaction medium is achieved through the addition of H_2O_2. Thus, H_2O_2 serves a double purpose in this case. The product of this reaction represents not only the result of the peroxidation of the second nonperoxo vanadium site on **1**, but also the full protonation of the citrate ligands attached to the arising $[V_2O_2(O)_2(O_2)_2]^0$ core in **5**.

Finally, complex $[V_2O_4(C_6H_4O_7)_2]^{6-}$ (**6**) was also shown to convert to complex **1** through appropriate acidification of the solution and addition of H_2O_2. Complex $(NH_4)_6[V_2O_4(C_6H_4O_7)_2]\cdot 6H_2O$ (**6**) had been synthesized, isolated, and fully characterized previously, both in the solid state as well as in solution.[28] The stoichiometric reaction is shown in reaction 7:

$$[V_2O_4(C_6H_4O_7)_2]^{6-}(\mathbf{6}) + H_2O_2 + 2H^+ \rightarrow [(VO_2)\{VO(O_2)\}(C_6H_5O_7)_2]^{4-}(\mathbf{1}) + H_2O \quad (7)$$

Here, acidification of the solution is promoted through the addition of HCl.

All of the above transformations led to crystalline products, which were positively identified by their FT-IR signatures and, on occasion, through unit-cell constant determination by X-ray crystallography. Beyond the significance of the investigated conversions involving complex **1** and the three complexes $(NH_4)_2[V_2O_4(C_6H_6O_7)_2]\cdot 2H_2O$ (pH ~3.5), $(NH_4)_4[V_2O_4(C_6H_5O_7)_2]\cdot 4H_2O$ (pH ~5), and $(NH_4)_6[V_2O_4(C_6H_4O_7)_2]\cdot 6H_2O$ (pH ~7.5), it appears that, from the synthetic point of view, the aforementioned transformations could serve as additional methods for the synthesis and isolation of such complexes from the dinuclear species $(NH_4)_4[(VO_2)\{VO(O_2)\}(C_6H_5O_7)_2]\cdot 1.5H_2O$ and vice versa.

Description of X-ray Crystallographic Structure of $(NH_4)_4[(VO_2)\{VO(O_2)\}(C_6H_5O_7)_2]\cdot 1.5H_2O$ (1). The X-ray crystal structure of **1** consists of discrete anions and ammonium (NH_4^+) cations. Complex **1** crystallizes in the monoclinic space group *I*2/*a*, with eight molecules in the unit cell. The structural diagram of the anion in **1** is shown in Figure 1. A list of selected interatomic distances and bond angles for **1** is provided in Table 2. The anionic complex in **1** consists of a $V^V{}_2O_2$ core with

dx.doi.org/10.1021/ic201204s |*Inorg. Chem.* 2011, 50, 11423–11436

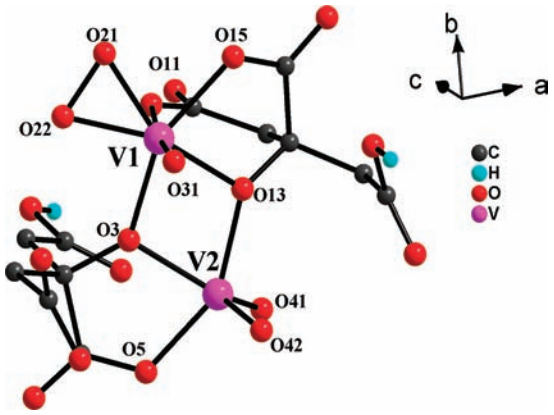

Figure 1. Partially labeled DIAMOND plot of the $[(VO_2)\{VO(O_2)\}(C_6H_5O_7)_2]^{4-}$ anion with the atom labeling scheme in $(NH_4)_4[(VO_2)\{VO(O_2)\}(C_6H_5O_7)_2]\cdot 1.5H_2O$ (**1**).

Table 2. Bond Lengths and Bond Angles for Compound 1

Bond Distances			
bond pairing	bond length (Å)	bond pairing	bond length (Å)
V(1)−O(31)	1.601(2)	V(1)−O(11)	2.266(2)
V(1)−O(22)	1.883(2)	V(2)−O(41)	1.621(3)
V(1)−O(21)	1.883(2)	V(2)−O(42)	1.628(2)
V(1)−O(13)	2.008(2)	V(2)−O(13)	1.977(2)
V(1)−O(3)	2.031(2)	V(2)−O(5)	1.988(2)
V(1)−O(15)	2.052(2)	V(2)−O(3)	2.008(2)

Bond Angles			
bond angle	value (deg)	bond angle	value (deg)
O(31)−V(1)−O(22)	101.4(1)	O(21)−V(1)−O(11)	83.1(1)
O(31)−V(1)−O(21)	100.3(1)	O(13)−V(1)−O(11)	78.3(1)
O(22)−V(1)−O(21)	44.1(1)	O(3)−V(1)−O(11)	85.3(1)
O(31)−V(1)−O(13)	96.3(1)	O(15)−V(1)−O(11)	80.8(1)
O(22)−V(1)−O(13)	152.6(1)	O(41)−V(2)−O(42)	107.4(1)
O(21)−V(1)−O(13)	150.9(1)	O(41)−V(2)−O(13)	100.0(1)
O(31)−V(1)−O(3)	96.6(1)	O(42)−V(2)−O(13)	98.3(1)
O(22)−V(1)−O(3)	85.5(1)	O(41)−V(2)−O(5)	99.6(1)
O(21)−V(1)−O(3)	129.0(1)	O(42)−V(2)−O(5)	97.4(1)
O(13)−V(1)−O(3)	71.7(1)	O(13)−V(2)−O(5)	149.9(1)
O(31)−V(1)−O(15)	94.4(1)	O(41)−V(2)−O(3)	119.4(1)
O(22)−V(1)−O(15)	121.8(1)	O(42)−V(2)−O(3)	133.1(1)
O(21)−V(1)−O(15)	78.1(1)	O(13)−V(2)−O(3)	72.9(1)
O(13)−V(1)−O(15)	77.0(1)	O(5)−V(2)−O(3)	77.6(1)
O(3)−V(1)−O(15)	147.8(1)	V(2)−O(3)−V(1)	105.3(1)
O(31)−V(1)−O(11)	173.5(1)	V(2)−O(13)−V(1)	107.4(1)
O(22)−V(1)−O(11)	84.9(1)		

the two V ions in the oxidation state +5. The rhombic core unit contains two oxygen bridges, which are derived from the alkoxide moieties of the two citrate ligands attached to the core. Each citrate participating in the coordination sphere around each V ion is triply deprotonated, i.e., only one of the terminal carboxylate groups in each citrate ligand is protonated. The two citrate ligands adopt different coordination modes. They both bind to the metal ions through the central alkoxide and carboxylate groups; the deprotonated terminal carboxylate group, however, of only one citrate ligand is bound to V(V), which belongs to the peroxo-V(V) center. In the nonperoxo-V(V) center, both terminal carboxylate groups abstain from coordination. As a result of the different ligation modes of the citrate ligands and the coordination of the peroxo group, the V ions present different coordination environments. Specifically, V(1) is coordinated to a doubly bonded oxygen (O(31)), to the peroxo-O atoms O(21) and O(22), to two alkoxide O atoms from the two citrate ligands (O(3) and O(13)), and to two carboxylato-O atoms (O(11) and O(15)). The coordination geometry around V(1) is pentagonal bipyramidal with atoms O(11) and O(31) in the apical positions. V(2) is coordinated to two doubly bonded O atoms O(41) and O(42), to the two bridging alkoxide O atoms O(3) and O(13), and to the carboxylato-O atom O(5). The coordination geometry around V(2) is distorted trigonal bipyramidal with atoms O(5) and O(13) in the apical positions ($\tau = 0.281$).

It should be emphasized that the uncoordinated terminal carboxylate groups of the two citrate ligands differ in their protonation state. This is a novel feature in the structural chemistry of V(V)-citrate dinuclear complexes, one that has been observed in only one other known complex (i.e., $K_4[V_2O_4(C_6H_5O_7)_2]\cdot 5.6H_2O$).[27] In all known cases of dinuclear V(V)-citrate complexes, the terminal carboxylates abstain from binding to the $V^V{}_2O_2$ core.

The V−O bond distances in **1** are similar to the corresponding distances in other V(V)-peroxo dimers, such as $(NH_4)_2[V_2O_2(O_2)_2(C_6H_6O_7)_2]\cdot 2H_2O$ (1.873(2)− 2.034(2) Å),[15] $K_2[V_2O_2(O_2)_2(C_6H_6O_7)_2]\cdot 2H_2O$ (1.873(1)− 2.039(1) Å),[29] $(NH_4)_4[V_2O_2(O_2)_2(C_4H_3O_5)_2]\cdot 3H_2O$ (1.859(3)− 2.294(3) Å),[30] $K_4[V_2O_2(O_2)_2(C_4H_3O_5)_2]\cdot 4H_2O$ (1.868(2)− 2.248(2) Å),[30] $K_2[V_2O_2(O_2)_2(C_4H_4O_5)_2]\cdot 2H_2O$ (1.869(2)− 2.033(2) Å),[30] and the nonperoxo species $K_4[V_2O_4(C_6H_5O_7)_2]\cdot 5.6H_2O$ (1.966(2)− 2.017(2) Å),[27] $Na_2[V_2O_4(C_6H_6O_7)_2]\cdot 2H_2O$ (1.957(3)− 2.000(3) Å),[15] $Cs_2[V_2O_4(C_4H_4O_5)_2]\cdot 2H_2O$ (1.963(4)− 2.016(4) Å),[31] $(NH_4)_2[V(O)_2(OC(CH_2CH_3)_2COO)]_2$ (1.973(1)− 1.984(2) Å),[32] and $Na_2[V_2O_4(C_4H_6O_3)_2]\cdot 7H_2O$ (1.990(1)− 2.004(1) Å).[33] The V═O bond distances (1.601(2)− 1.628(2) Å) are similar to those in the congener complex $K_4[V_2O_4(C_6H_5O_7)_2]\cdot 5.6H_2O$ (1.618(3)− 1.634(3) Å). The angles in **1** are similar to those observed in many $V^V{}_2O_2$ core-containing dimers, exhibiting distorted trigonal bipyramidal and pentagonal bipyramidal geometry of the bound citrates around the V(V) ions.[15,19,27]

The citrate ligands in the anion of **1** adopt an extended conformation upon binding to the V(V) ion. The C atoms C(1), C(2), C(3), C(5), and C(6) of the citrate backbone are coplanar, with the largest standard deviation being 0.05 Å for C(2); the corresponding value for the second citrate ligand is 0.09 Å for C(16). The central carboxylate plane O(4)−C(4)−O(5) is rotated 1.3° out of the O(3)−C(3)−C(4) plane (12.3° for the second citrate ligand). These values are consistent with those seen in other V(V)-citrate complexes, suggesting a similar approach of the citrate to the metal ion in all cases of complex assemblies.[27] The V···V distance in the anion of **1** is 3.212(1) Å. This value is similar to those observed in V(V)-citrate dinuclear complexes described above and reported previously.

The protonated terminal carboxylate groups are involved in strong intermolecular hydrogen bonding interactions of two types: (a) the double O1−H1O···O2 bonds create dimers of dimers of **1**, and (b) the O17−H17O···O7 bonds connect the

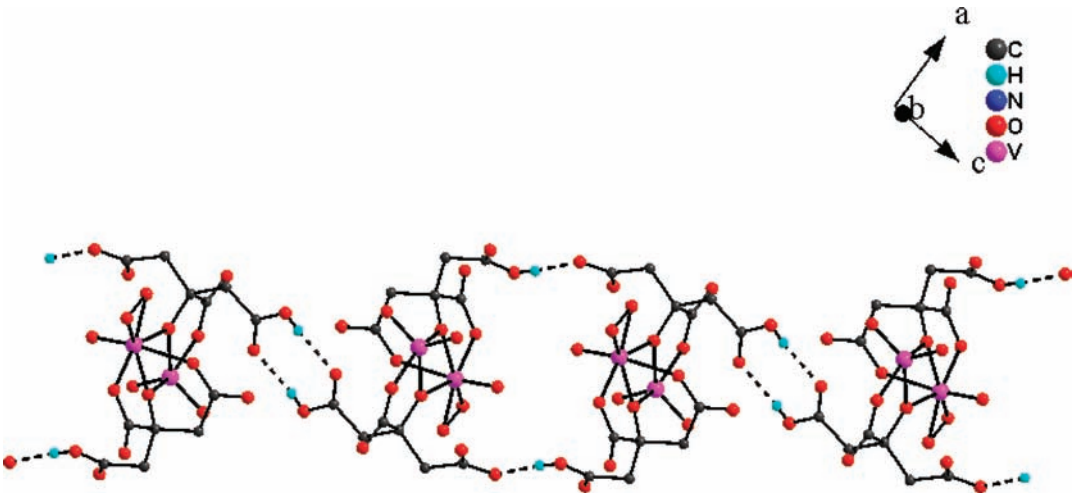

Figure 2. Plot of a small fragment of the one-dimensional (1D) anionic chains of **1** due to hydrogen bonding interactions (dashed lines).

dimers into one-dimensional (1D) anionic chains extending parallel to the ($\bar{1}$01) crystallographic plane (see Figure 2 and Table 3).

Four ammonium counterions are present in **1**. They counterbalance the 4− charge generated on the complex anion. The cations are in contact with the carboxylate oxygens of the citrate anion, as well as the VO_2^+ oxo and the peroxo group, and the lattice water oxygens. The presence of water molecules of crystallization in **1** may aid in the formation of an extensive hydrogen-bonding network (Table 3) in the lattice of **1**.

UV−Visible Spectroscopy. The electronic spectrum of **1** was recorded in H_2O. The spectrum exhibits a band at 415 nm (ε = 430 M^{-1} cm^{-1}) with a rising absorbance into the UV region. An additional feature appears at ∼241 nm (ε = 6000 M^{-1} cm^{-1}). The spectrum is featureless beyond 450 nm. The band at 415 nm has been attributed to the presence of a peroxo-to-vanadium ligand-to-metal charge-transfer (LMCT) transition.[34] Thus, under the prevailing pH conditions investigated, the peroxo moiety is attached to the V(V) ion. The latter contention is supported by the presence of a similar LMCT absorption at 340 nm in complex $(NH_4)_4[V_2O_2(O_2)_2(C_4H_3O_5)_2]\cdot 3H_2O$,[30a] lending credence to the idea of a stable $[(V{=}O)(O_2)]^+$ unit in this class of complexes. The presence of the weak LMCT band[35] was also observed in other vanadium−peroxo citrate complexes containing a $[(V{=}O)_2O_2(O_2)_2]^0$ core[14,16,17] and was reasonably attributed to a $\pi_v^* \rightarrow$ d transition.[34,35] The intense absorption band at 241 nm in **1**, in the UV region, may be associated with a $\pi_h^* \rightarrow$ dσ^* LMCT transition. This transition had been previously proposed to exist at energies higher than the $\pi_v^* \rightarrow$ d transition, because of the stabilization of the $\pi_h^*\sigma$ peroxo-to-metal bonding orbital. Currently, detailed definitive assignments cannot be made, because of the absence of pertinent spectroscopic studies.

FT-IR Spectroscopy. The FT-IR spectra of **1** in KBr revealed the presence of vibrationally active carboxylate groups. Antisymmetric and symmetric vibrations for the carboxylate groups of the coordinated citrate ligands dominated the spectra. Specifically, antisymmetric stretching vibrations $\nu_{as}(COO^-)$ were present for the carboxylate carbonyls in the range of 1710−1632 cm^{-1}. Symmetric vibrations $\nu_s(COO^-)$ for the same groups were present at ∼1398 cm^{-1}. The carbonyl vibrations were shifted to lower frequency values, in comparison to the corresponding vibrations in free citric acid, suggesting changes in the vibrational status of the citrate ligand that is coordinated to the vanadium.[36] The difference between the symmetric and antisymmetric stretches, $\Delta(\nu_{as}(COO^-)-\nu_s(COO^-))$, was >200 cm^{-1}, indicating that the carboxylate groups in the citrates were either free or coordinated to vanadium in a monodentate fashion.[21] The latter contention was confirmed by the X-ray crystal structure of **1**. Furthermore, the ν(V=O) vibration for the $VO(O_2)^+$ group in **1** was present at ∼951 cm^{-1}. The peroxo ν(O−O) stretch was attributed to vibrations at 931 cm^{-1}. In addition, the $\nu(VO_2^+)$ vibrations for the VO_2^+ groups in **1** were present in the range of 914−873 cm^{-1}. The described tentative assignments were consistent with previous reports on dinuclear V(V) complexes,[14,15,30b,37,38] and were also consistent with previously reported infrared frequencies that are attributed to carboxylate-containing ligands bound to various metal ions.[39]

Raman Spectroscopy. Complex **1** was characterized by FT-Raman spectroscopy. Vibrational spectroscopy has already been successfully utilized to characterize vanadium peroxo complexes.[40−42] Typical bands assigned to V=O, V−O_p (peroxo), and O−O vibrations in V(V)-peroxo complexes are observed[39−41] in the spectral windows of 920−1000, 660−440, and 800−950 cm^{-1}, respectively. The FT-Raman spectrum of **1** is shown in Figure 3. The main spectral features of O−O and V=O stretching are separately shown in the inset. The strong scattering peak at 942 cm^{-1} and the Raman band at ∼924 cm^{-1} are respectively attributed to the V=O and O−O stretching of the $VO(O_2)$ group in typical monoperoxo−V complexes.[41,43] The corresponding V−O_p stretching features appear in the spectral region of 530−625 cm^{-1}. The Raman peak situated at 961 cm^{-1} is attributed to the V=O stretch of the VO_2 moiety;[44−46] the high frequency shift is mostly due to a reduction in the V(V) coordination number, thereby reinforcing the V−O bond.[43] The Raman bands at 1415 and 2931 cm^{-1} are assigned to the bending and stretching vibrational modes of the methylene groups, respectively.

Solid-State NMR Spectroscopy. The CP-MAS ^{13}C NMR spectra of **1** (Figure 4A) in the solid state reveals the presence of coordinated citrate to V(V). Specifically, the spectrum shows separate resonances for the various carbons of the citrate ligand and exhibits a distinctly different pattern compared to free citric acid.[39e] Two types of those signals lie in the high-field region, whereas the others emerge in the low-field region of the spectrum. The group of resonances in the high-field region could

Table 3. Hydrogen Bonds in Compound 1

	Bond Lengths (Å)		Bond Angle (deg)	
interaction	D···A	H···A	D−H···A	symmetry operation
O1−H1O···O2	2.656	1.922	174.3	$-x, -y, -z$
O17−H17O···O7	2.496	1.690	171.8	$0.5 - x, 0.5 - y, 0.5 - z$
N1−H1NA···O31	2.988	2.332	139.2	$-x, 0.5 + y, 0.5 - z$
N1−H1NB···O4	2.839	1.925	168.9	x, y, z
N1−H1NC···O14	2.839	2.049	153.1	$-0.5 + x, -y, z$
N1−H1ND···O16	2.825	1.934	158.0	$-0.5 + x, 1 - y, z$
N2−H2NA···O6	2.750	1.933	161.0	$-x, -1 + y, z$
N2−H2NB···O15	3.010	2.349	141.0	$0.5 - x, -0.5 - y, 0.5 - z$
N2−H2NB···O31	3.005	2.383	135.8	$0.5 - x, -0.5 - y, 0.5 - z$
N2−H2NC···O15	3.037	2.130	164.4	x, y, z
N2−H2NC···O21	2.976	2.334	125.8	x, y, z
N2−H2ND···O41	2.868	2.000	163.1	$x, -1 + y, z$
N3−H3NA···O6	2.944	2.123	170.0	$x, -1 + y, z$
N3−H3NB···O7	2.837	1.995	173.0	$-x, -0.5 + y, 0.5 - z$
N3−H3NC···O4	2.843	2.358	117.2	$x, -1 + y, z$
N3−H3NC···O2wB	3.275	2.454	165.4	$-x, -0.5 + y, 0.5 - z$
N3−H3ND···O11	2.730	1.893	170.3	x, y, z
N4−H4NA···O2wB	3.171	2.417	157.5	$x, -0.5 - y, -0.5 + z$
N4−H4NB···O1w	2.779	2.350	114.4	$x, -1 + y, z$
N4−H4NC···O14	2.889	2.170	146.0	$-x, -y, -z$
N4−H4ND···O12	2.764	1.959	156.3	x, y, z

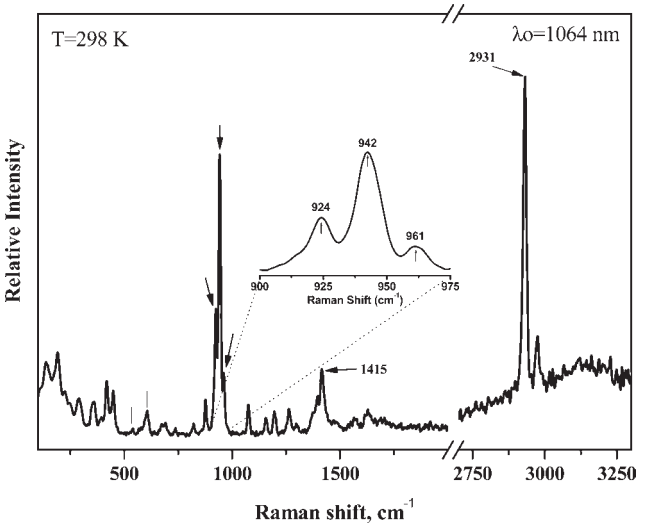

Figure 3. Raman spectrum of **1**.

be attributed to the methylene carbons (44.0−50.0 ppm) located adjacent to the coordinated carboxylates of the citrate ligand. The signal at 88.0 ppm is reasonably attributed to the central C atom located adjacent to the bound central carboxylate group. In the low-field region, where the carbonyl carbon resonances are expected, there were broad resonances in the region of 180.0−185.0 ppm, attributable to the carboxylate groups (central and terminal). Specifically, the resonance located at 180.0 ppm is attributable to the terminal carboxylate carbon, while the resonance at the low end of the field (185.0 ppm) is attributed to the central carboxylate carbon attached to the V(V) ion. This signal is shifted to lower fields, in comparison to the terminal carboxylate carbon signal. The shift is most likely due to the presence of the central carboxylate carbon being close to the deprotonated alkoxide group of the V(V) bound citrates.

^{51}V has a spin of $^{7}/_{2}$, which is a fact that has been reportedly exploited to gain knowledge on the structural features of V(V) compounds.[47] The ^{51}V MAS NMR spectrum of **1** is shown in Figure 5. It exhibits multiple spinning sidebands as a result of both quadrupolar coupling and chemical shift anisotropy. Since the signals show normal Gaussian shape, only quadrupolar coupling to the first order is effective. The spectrum of **1** exhibits two isotropic signals, at −557 and −589 ppm, with a small signal at −540 ppm, that might indicate decomposition under the measurement conditions. Therefore, only 128 scans were taken and full simulation (see below) is only carried out for the −589 ppm signal. Assignments of NMR shifts to different coordination numbers of V(V) compounds are not straightforward.[48] Based on previous reports on several known compounds,[49] various patterns have been observed, earmarking specific regions in the ^{51}V spectrum for 5-, 6-, and 7-coordinated V(V) ions. The solid-state ^{51}V NMR analysis is very sensitive, even to small angle changes in the observed geometry around vanadium. Consistent with the above information, 5-coordinated V(V) compounds exhibit resonances in the range of −350 ppm and −500 ppm and 7-coordinated V(V) compounds exhibit resonances in the range between −500 ppm and −700 ppm. There might be a large overlap between ranges, but within a single species bearing V(V) centers with different coordination numbers, a trend toward more negative shifts would be expected for higher coordination numbers. Tentatively, the lower field in the spectrum of **1** could be assigned to the 5-coordinated V(V) and the higher field could be assigned to the 7-coordinated V(V) center. Based approximately on the intensities

dx.doi.org/10.1021/ic201204s |*Inorg. Chem.* 2011, 50, 11423–11436

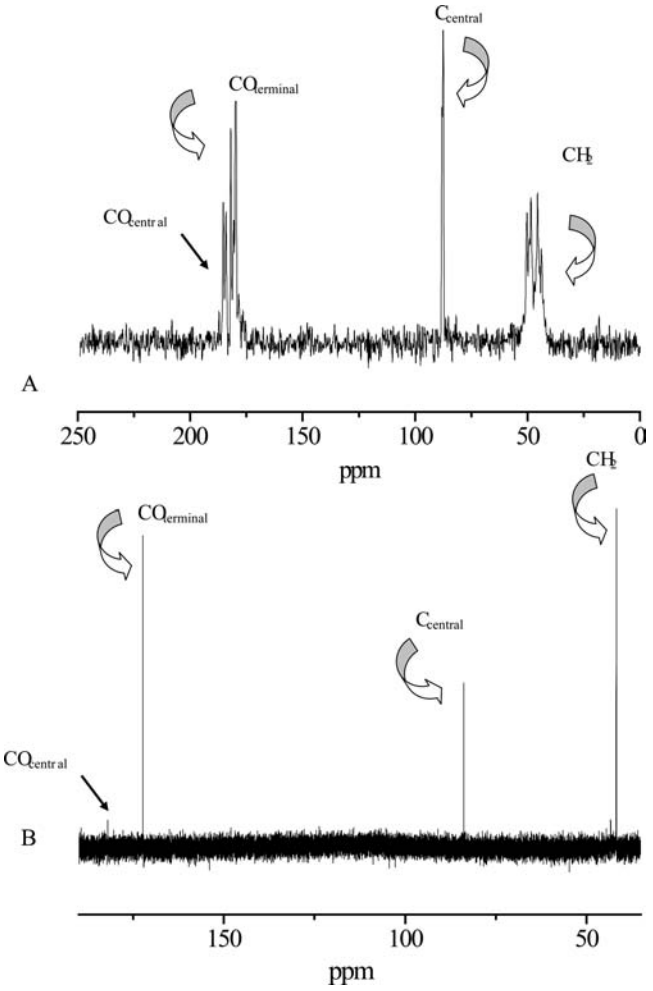

Figure 4. (A) Solid-state CP-MAS ^{13}C NMR spectrum of **1**. (B) ^{13}C NMR spectrum of **1** in D_2O.

observed, a 1:1 ratio of the two V(V) signals is observed in the case of the main signals of the spectrum of **1**.

Simulations for the −589 ppm signal were performed with the SIMPSON[50] program by varying quadrupolar coupling and asymmetry parameters to obtain the best fit. The parameters for the chemical shift anisotropy (CSA) were predetermined by simulating the sideband intensities around the isotropic signal using Dmfit,[51] which showed good agreement with the experimental data. The angular relation of CSA and the quadrupolar tensor is not given, in view of the fact that only small changes to the sideband intensities were observed and are not reliable, with regard to the signal-to-noise ratio. The simulated spectrum was convoluted through a Lorentzian shape of 300 kHz fwhh (full width at half height), to accommodate the pulse excitation and probe bandwidth. The simulated spectrum is also included in Figure 5. The obtained parameters are $\Delta\delta$ = −700 ppm, η_σ = 0.5, C_Q = 7 MHz, and η_Q = 0.1. For the −557 ppm signal, due to low signal intensity (see above), only the CSA was determined from the intensity of the spinning sidebands, using the Dmfit program.[51] The parameters—$\Delta\delta$ = −700 ppm and η_σ = 0.5—are similar to those of the −589 ppm signal. The uncertainty is lower, because of the influence of the (not-resolved) sidebands from first-order quadrupolar coupling. Further work into the MAS ^{51}V NMR on this and other congener dinuclear vanadium species of citrate is currently underway.

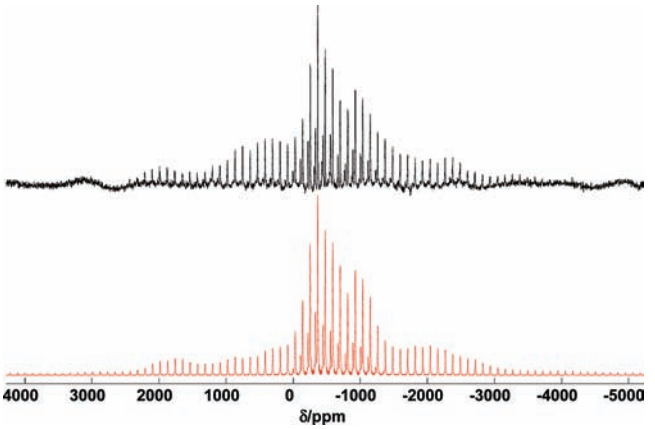

Figure 5. MAS ^{51}V NMR experimental spectrum of **1** (top, black) together with the simulation (bottom, red). For the signal at −589 ppm, chemical shift anisotropy (CSA) and quadrupolar coupling were taken into account, whereas for the −557 ppm signal, only CSA was considered (see text).

Solution NMR Spectroscopy. The solution ^{13}C NMR spectrum of complex **1** was measured in D_2O (Figure 4B). The spectrum reveals the presence of several resonances. The resonance in the high-field region (41.7 ppm) is attributed to the CH_2 groups of the citrate ligands bound to the central V(V) ion of the dinuclear V_2O_2 core. The resonance at 83.9 ppm is assigned to the central carbon of the bound citrate. Signals at 172.3 ppm in the lower-field region were assigned to the terminal carboxylate carbons. The resonance located at the low end of the field, 182.0 ppm, is attributed to the central carboxylate carbon attached to the V(V) ion. This signal is shifted to lower fields, in comparison to the terminal carboxylate carbon signal. In this case as well, the shift is most likely due to the presence of the central carboxylate carbon being close to the deprotonated alkoxide group of the V(V) bound citrates. The pattern of resonances observed is similar to that observed in the CP-MAS ^{13}C NMR analysis of the same material **1**, which is consistent with the structural composition of the compound.

Cyclic Voltammetry. The cyclic voltammetry of complex **1** was studied in aqueous solutions, in the presence of KNO_3 as a supporting electrolyte (see Figure 1S in the Supporting Information section). The cyclic voltammogram of **1** (scan rate = 100 mV/s) exhibits ill-defined electrochemical behavior, with a reduction wave at E_{pc} = −618 mV, followed by an oxidation wave at E_{pa} = −442 mV. This voltammetric behavior likely projects irreversible sequential V(V)/V(IV) redox processes associated with species **1**. The observed irreversibility may reflect complex electrochemical processes, involving concurrent redox state and coordination number changes associated with the presence/absence of peroxide on the V_2O_2 core bound to citrate (vide infra). Attempts to pursue the isolation of reduced products of **1** are currently ongoing.

DISCUSSION

Diverse Synthetic Aqueous V(V)−Peroxo-citrate Chemistry. The aqueous synthetic chemistry of binary vanadium-citrate and ternary vanadium-peroxo-citrate systems has afforded several dinuclear complexes with variable structural features and chemical reactivity attributes.[14,16,17,30b] In several synthetic reactions covering relevant conditions, simple reagents were

employed to obtain discrete complexes crystallizing out of aqueous media. In this sense, V(V) (V_2O_5), as well as V(III) (VCl_3), were used as starting materials for the synthesis of a novel V(V)-peroxo-citrate complex. Under specific pH conditions, non-redox as well as redox chemistry, developed in the presence of the physiologically relevant citric acid and hydrogen peroxide, led to the synthesis and ultimate isolation of a new and unique mixed V(V)-peroxo-citrate complex, $(NH_4)_4[(VO_2)\{VO(O_2)\}(C_6H_5O_7)_2]\cdot 1.5H_2O$ (**1**).

The analytical, spectroscopic (FT-IR, Raman, NMR), electrochemical, and structural (X-ray crystallographic) features observed in **1** are true attributes of dinuclear complexes containing a full complement of either VO_2^+ or $VO(O_2)^+$ moieties alongside the coordinated citrate ligands.[14−17,29,30b] These moieties are reminiscent of corresponding V_2O_2 scaffold-containing homodinuclear complexes, such as $[V_2O_4(C_6H_6O_7)_2]^{2-}$, $[V_2O_4(C_6H_5O_7)_2]^{4-}$,[27] and $[V_2O_4(C_6H_4O_7)_2]^{6-}$,[22] containing the VO_2^+ unit, and V(V)-peroxo-citrate congener species, such as $(NH_4)_2[V_2O_2(O_2)_2(C_6H_6O_7)]_2\cdot 2H_2O$ and $(CH_6N_3)_4[V_2O_2(O_2)_2(C_6H_5O_7)_2]\cdot 6H_2O$ (**7**), bearing the $VO(O_2)^+$ unit. In this respect, it appears that complex **1** is an asymmetric assembly of half structural vanadium units originating in the aforementioned complexes. Specifically, the coordination number and geometry of the non-peroxo structural half of the $V^V_2O_2$ core are consistent with those observed in complexes **3**, **4**, and **6**. Similarly, the coordination number and geometry of the peroxo structural half of the assembly are consistent with those previously seen in **7**. Furthermore, the coordination mode and protonation state of the two citrate ligands bound to the corresponding halves of the anionic assembly emerge with distinct attributes. In the nonperoxo half, the citrate ligand exhibits a coordination mode identical to that seen in the complex $[V_2O_4(C_6H_5O_7)_2]^{4-}$,[27,28] with both terminal carboxylate groups (regardless of their protonation state) abstaining from binding to the core. In the peroxo half of the complex anion, the citrate ligand exhibits a coordination mode and protonation state identical to that observed in the $[V_2O_2(O_2)_2(C_6H_5O_7)_2]^{4-}$ component complex of the aggregate assembly species $K_{10}[V_2O_2(O_2)_2(C_6H_5O_7)_2][V_2O_2(O_2)_2(C_6H_4O_7)_2]\cdot 20H_2O$,[16] and the recently synthesized and characterized dinuclear species $(CH_6N_3)_4[V_2O_2(O_2)_2(C_6H_5O_7)_2]\cdot 6H_2O$ (**7**). In this half, the deprotonated carboxylate group binds V(V), whereas the protonated terminal carboxylate group stands away from the coordination environment of the V(V)−peroxo center.[30]

Based on the aforementioned structural features, the anion in **1** stands as an intermediate in the process of addition of the O_2^{2-} moiety onto the non-peroxo $[(VO_2)_2O_2]$ core upon reaction of the latter with H_2O_2. Specifically, when $[V_2O_4(C_6H_5O_7)_2]^{4-}$ reacts with H_2O_2, under the pH-specific aqueous conditions described in the herein presented work, one peroxo group is inserted into the basic V_2O_2 core, which is reflected in the isolated complex anion. The assembled anion, in combination with the employed ammonium cation, facilitated the isolation of **1** in the presence of the precipitating alcohol. Further addition of H_2O_2 to **1** leads to the anion in complex **7**, with the latter species representing the fully peroxidized dinuclear assembly. Subsequent addition of H_2O_2 to **7** leads to the ultimate isolation of **5**, thereby attesting to the acidifying ability of that agent protonating one of the carboxy terminals of the citrate ligand bound to each vanadium center. The specific contention, confirmed by the X-ray structure of **7** and **5**, renders **1** a potential intermediate in the reaction pathway leading from **3** to **5**.

It is worth emphasizing that, in the reaction pathway from **3** to **5** through complex **1**, the key species involved and identified contain the ammonium ion as a counterion. The fact that there was a common counterion in all of the synthetic process involved helped unravel the described potential reaction pathway. To this end, it appears that ammonium may have been the appropriate cation to use in this reaction chemistry in order to isolate complex **1** under the employed experimental conditions. Attempts to pursue the synthesis and isolation of the corresponding assembly of **1** in the presence of a different counterion, such as potassium (K^+), did not result in the isolation of the corresponding complex. The importance of the cation in the synthesis and isolation of discrete vanadium-citrate complexes is actually not new. It has been noted previously and emphasized in the case of complex $[V_2O_4(C_6H_4O_7)_2]^{6-}$, where only the ammonium salt of that anion could be isolated in a crystalline form. In contrast, efforts to isolate the potassium salt of the same anion were not successful. Consequently, the cation specific chemistry explored here was crucial in unraveling the nature of complex **1** and its involvement in the reaction pathway leading from **3** to **5**. Collectively, it appears that the seemingly simple synthetic reactions employed for the synthesis of various ternary V(V)-peroxo-citrate or other V(V)-peroxo-hydroxycarboxylate complexes prove to be quite complex, in that they involve various stages and intermediates that now emerge characterized.

Structural Diversity of V(V)−Peroxo-citrate Species through Interconversions. Complex **1** displays a widely diverse reactivity in the presence of H_2O_2, and under thermal as well as nonthermal transformation conditions (see Figure 6 and Figure 2S in the Supporting Information). As a potential intermediate in the reaction pathway leading from complex **3** to complex **5**, its association with both complexes was investigated and established. In particular, the conversion of **1** toward complex **3** was promoted through simple stirring of its solutions under mild heating for a brief period of time. It basically showed that (a) the peroxide group can easily be detached from the complex, and (b) aqueous solutions of peroxo-containing dinuclear complexes are not very stable at room temperature for long periods of time. The reverse conversion of **3** to **1** was effected through the addition of H_2O_2 in a pH-specific manner. Thus, a reversible interconversion between **1** and **5** was amply established, simultaneously rendering **1** as a first-step intermediate in the addition of peroxide to **3**. In another transformation, solutions of **1** stirred at room temperature for hours afforded the complex $(NH_4)_2[V_2O_4(C_6H_6O_7)_2]\cdot 2H_2O$ (**4**). Note that both **3** and **4** had been previously shown to connect to complex **5** through H_2O_2 reactions, under appropriately selected conditions.

In an aptly efficient manner, the addition of H_2O_2 to solutions of pure **1** resulted in the formation and isolation of complex **5**, which is the fully peroxidized form of a dinuclear complex. This form had been independently synthesized previously, isolated from aqueous solutions and spectroscopically and structurally characterized.[29,15] Thus, the intermediate character of **1** in the route leading to **5** had been shown. The importance of **1** as a discrete species in the maze of V(V)-peroxo-citrate reactivity was also shown through pH adjustment and the ensuing addition of H_2O_2 to aqueous solutions of $(NH_4)_6[V_2O_4(C_6H_4O_7)_2]\cdot 6H_2O$ (**6**). Thus, all three dinuclear nonperoxo V(V)-citrate complexes **3**, **4**, and **6** could serve as initial points toward the synthesis and isolation of complex **1**. It is worth mentioning that all three complexes **3**, **4**, and **6** had been previously shown to be active participants in the aqueous structural V(V)-citrate speciation.

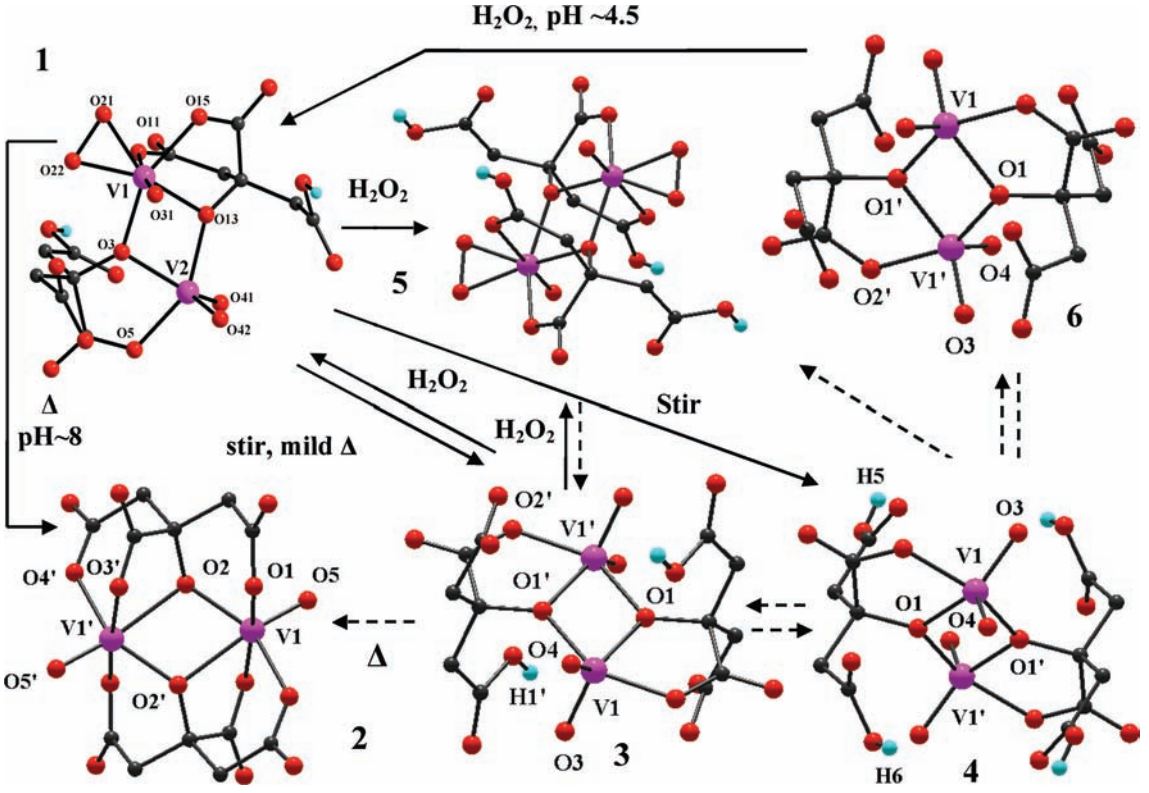

Figure 6. Scheme of pH-dependent and thermal transformations among various V(IV,V)-citrate anionic complexes. Dashed arrows reflect previously established interconversions between vanadium-citrate species.

In an as-yet-significant thermal transformation, complex **1** converted to complex **2** under heating and pH adjustment to ~8. In an analogous manner, complexes **3**, **4**, **5**, and **6** were also shown to convert to **2** through heating of their aqueous solutions. The blue solution of complex **2** was undoubtedly indicative of the oxidation state +4 of the V ions involved in the homodinuclear V(IV) product complex. In view of the fact that the starting material contained V(V) and the produced species **2** contained V(IV), it appears that a reduction had taken place. This reduction had been seen previously with other metal carboxylate species and attributed to the oxidative decarboxylation of citrate by V(V).[52]

Based on the aforementioned transformations originating from or leading up to **1**, it appears that the universally constant structural feature in all involved dinuclear complexes is the V_2O_2 core. The unique case of **1** containing one-half of a $[(VO_2)_2O_2]^0$ core of a nonperoxo dinuclear complex and one-half of a $[(VO)_2O_2(O_2)_2]^0$ core of a peroxo dinuclear complex lends credence to the previous statement and further supports the stability of the derived mixed $[(VO_2)\{(VO)(O_2)\}O_2]^0$ core.

V(V)−Peroxidation, Structural Diversity, and Potential Links to Biological Activity. The chemistry described in this work has led to several key conclusions about the aqueous V(V)-peroxo-citrate reactivity and associated species. In particular:

(1) Dinuclear complexes of V(V) bearing peroxide and citrate are widely spread in aqueous media of variable pH. The $V^V_2O_2$ core emerges not only during the synthetic processes, leading to specific dinuclear species, but also during transformations through/to other congener species. To this end, the rhombic core arises as a prominent feature consistent with past solution speciation studies, portending the presence of V(V)-citrate species containing dinuclear V_2O_2 cores (albeit not identical to those observed in the synthetic complexes).[53]

(2) Dinuclear complexes bearing one and/or two peroxo groups (one on each V(V) ion) can be isolated from aqueous media of the V(V)−H_2O_2−citrate ternary system. For the first time, it is shown that peroxo groups can be added to adjacently located vanadium ions in a stepwise sequential fashion, without affecting the basic V_2O_2 core of the complex (Figure 7).

The isolation and further crystallographic characterization of **1** proves that the only changes that occur are those associated with the coordination number and geometry around each vanadium center reacting with H_2O_2. That is also consistent with V(V)-peroxo-citrate homodinuclear complexes that have been isolated previously and structurally characterized. The sequential addition of peroxo groups to V(V) ions provides further clues on the diverse species that might exist in the aqueous distributions of the V(V)-peroxo-citrate system. In fact, it may suggest that other species could exist in the proposed pathway leading from **3** to **5** that are presently not known and elude detection and characterization. One such potential family of species could include dinuclear complexes like **5**, with an odd number (one or three) of terminal carboxylate groups on the citrate ligands bound to the V_2O_2 core being deprotonated. Analogous species could arise in the case of **1** and **7**. The emergence of such species is in line with previously synthesized binary and ternary V(IV,V)-citrate and V(V)-citrate-peroxo complexes, reflecting pH-structural variants in the respective aqueous speciation schemes.[14−16,21,27−30b] The aforementioned species could serve as precursors to complex **5** upon further acidification of the solution. They may indeed occur in our case due to the presence of H_2O_2 in

dx.doi.org/10.1021/ic201204s |*Inorg. Chem.* 2011, 50, 11423–11436

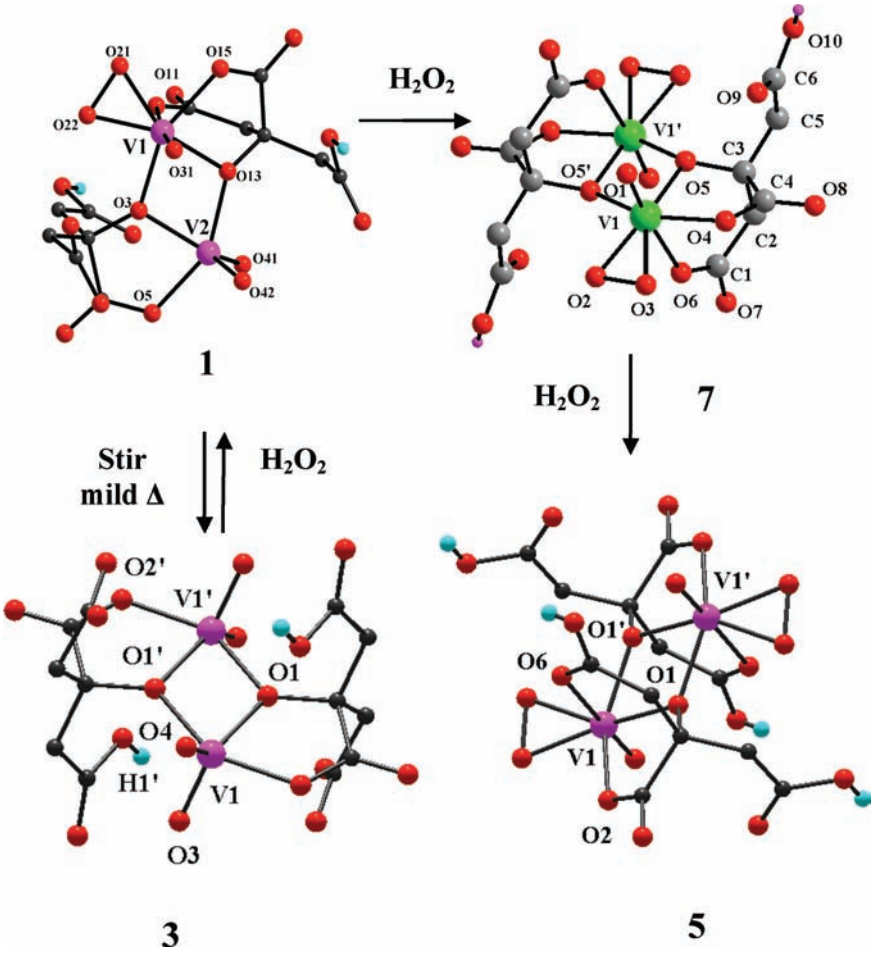

Figure 7. Tentative reaction pathway of the addition of H_2O_2 to V(V)-citrate dinuclear complexes.

the reaction medium, leading from **1** to **5**. The structural diversity observed among the species participating in the scheme outlined in this work may reflect a potentially diversified biological activity for the vanadium species in binary and ternary systems. Of specific value is the fact that dinuclear complexes can carry one and/or two peroxo groups on the core V ions. In a biological setting, where adjacently located V ions (either in abutting positions or linked as in the case of the dinuclear complexes discussed here) are subject to peroxidation, discrete species could arise with variable activity toward adjoining cellular targets, depending on the degree of peroxidation. In this sense, there may be a potential link between the degree of peroxidation and the arising (bio)chemical activity of the associated V ions. However, such a hypothesis is in need of further perusal at the (bio)chemical level. Vanadium-peroxo species have been shown to exhibit variable biological activity extending to antitumorigenicity[6] and insulin mimesis.[9−11,30b,54] Therefore, it remains to be seen whether the degree of peroxidation for a specific vanadium site begets analogously regulated and/or finely tuned activity for (bio)-chemically involved vanadium species.

CONCLUSIONS

The synthetic and transformation chemistry in the present work, and the interconnectivity between pairs of peroxo and nonperoxo vanadium species with (a) variable oxidation states for vanadium, (b) varying ligand protonation and modes of binding to vanadium ions in dinuclear complexes, and (c) a V_2O_2 core structure bearing the variably bound citrates, project an intricate structural speciation in binary and ternary vanadium systems with physiological ligands. Given the fact that solubility enhances bioavailability, the citrate chemistry of vanadium supports the plethoric speciation of that element in the presence of the physiologically relevant citrate and hydrogen peroxide (H_2O_2), and it projects soluble species that might be or become bioavailable under biologically relevant conditions. Therefore, the well-defined chemical and structural properties of such species constitute a basis of assessing their biological potential and enhance our understanding of the role of vanadium-specific reactivities in the respective media. In view of the fact that species with those features emerge under specific synthetic conditions, efforts to (a) pursue their synthesis and isolation and (b) relate them chemically and mechanistically to purported (bio)chemical interactions of vanadium are needed. Research geared toward these goals is currently ongoing in our laboratories.

ASSOCIATED CONTENT

Supporting Information. X-ray crystal crystallographic files, in CIF format, and listings of positional and thermal parameters and H-bond distances and angles for **1**. Cyclic voltammetry figure for **1**. The material is available free of charge via Internet at http://pubs.acs.org.

AUTHOR INFORMATION

Corresponding Author

*Tel.: +30-2310-996-179. Fax: +30-2310-996-196. E-mail: salif@auth.gr.

ACKNOWLEDGMENT

This work was supported by the Greek State Scholarships Foundation "IKY". The authors would like to thank the DFG (Deutsche Forschungsgemeinschaft) and the Experimental Physics Institutes of the Leipzig University for support (Dr. Bertmer) with the Avance 750 MHz NMR spectrometer.

REFERENCES

(1) (a) Rehder, D. *Bioinorganic Vanadium Chemistry*; Inorganic Chemistry: A Wiley Textbook Series; Wiley: New York, 2008. (b) Rehder, D. *Org. Biomol. Chem.* **2008**, *6*, 957–964. (c) Baran, E. J. *J. Inorg. Biochem.* **2000**, *80*, 1–10. (d) Zubieta, J. *Comments Inorg. Chem.* **1994**, *3*, 153–183. (e) Chen, Q.; Salta, J.; Zubieta, J. *Inorg. Chem.* **1993**, *32*, 4485–4486. (f) Rehder, D. *Angew. Chem., Int. Ed. Engl.* **1991**, *30*, 148–167.

(2) (a) Bayer, E. In *Amavadin, the Vanadium Compound of Amanitae*; Sigel, H., Sigel, A., Eds.; Metal Ions in Biological Systems, Vol. 31; Marcel Dekker: New York, 1995; Chapter 12, pp 407−421. (b) Smith, M. J.; Ryan, D. E.; Nakanishi, K.; Frank, P.; Hodgson, K. O. In *Vanadium in Ascidians and the Chemistry in Tunichromes*; Sigel, H., Sigel, A., Eds.; Metal Ions in Biological Systems, Vol. 31; Marcel Dekker: New York, 1995; Chapter 13, pp 423−490. (c) Frausto da Silva, J. J. R. *Chem. Speciation Bioavailability* **1989**, *1*, 139–150.

(3) (a) Weyand, M.; Hecht, H.; Kiess, M.; Liaud, M.; Vilter, H.; Schomburg, D. *J. Mol. Biol.* **1999**, *293*, 595–611.(b) Vilter, H. In *Vanadium and Its Role in Life*; Sigel, H., Sigel, A., Eds.; Metal Ions in Biological Systems, Vol. 31; Marcel Dekker: New York, 1995; Chapter 10, pp 325−362. (c) Butler, A. *Curr. Opin. Chem. Biol.* **1998**, *2*, 279–285.

(4) Liang, J.; Madden, M.; Shah, V. K.; Burris, R. H. *Biochemistry* **1990**, *29*, 8577–8581.

(5) (a) Smith, B. E.; Durrant, M. C.; Faihurst, S. A.; Gormal, C. A.; Grönberg, K. L. C.; Henderson, R. A.; Ibrahim, S. K.; Le Gall, T.; Pickett, C. J. *Coord. Chem. Rev.* **1999**, *185−186*, 669–687. (b) Grönberg, K. L. C.; Gormal, C. A.; Durrant, M. C.; Smith, B. E.; Henderson, R. A. *J. Am. Chem. Soc.* **1998**, *120*, 10613–10621. (c) Howard, J. B.; Rees, D. C. *Chem. Rev.* **1996**, *96*, 2965–2982.

(6) (a) Djordjevic, C. In *Antitumorigenic Activity of Vanadium Compounds*; Sigel, H., Sigel, A., Eds.; Metal Ions in Biological Systems, Vol. 31; Marcel Dekker: New York, 1995; Chapter 18, pp 595−616. (b) Köpf-Maier, P.; Köpf, H. In *Metal Compounds in Cancer Therapy*; Fricker, S. P., Ed.; Chapman and Hall: London, 1994; pp 109−146. (c) Djordjevic, C.; Wampler, G. L. *J. Inorg. Biochem.* **1985**, *25*, 51.

(7) (a) Klarlund, J. K. *Cell* **1985**, *41*, 707–717. (b) Smith, J. B. *Proc. Natl. Acad. Sci. U.S.A.* **1983**, *80*, 6162–6167.

(8) (a) Walton, K. M.; Dixon, J. E. *Annu. Rev. Biochem.* **1993**, *62*, 101–120. (b) Lau, K.-H. W.; Farley, J. R.; Baylink, D. J. *Biochem. J.* **1989**, *257*, 23–36.

(9) (a) Brand, R. M.; Hamel, F. G. *Int. J. Pharm.* **1999**, *183*, 117–123. (b) Drake, P. G.; Posner, B. I. *Mol. Cell. Biochem.* **1998**, *182*, 79–89. (c) Drake, P. G.; Bevan, A. P.; Burgess, J. W.; Bergeron, J. J.; Posner, B. I. *Endocrinology* **1996**, *137*, 4960–4968. (d) Eriksson, J. W.; Lonnroth, P.; Posner, B. I.; Shaver, A.; Wesslau, C.; Smith, U. P. *Diabetologia* **1996**, *39*, 235–242.(e) Stankiewicz, P. J.; Tracey, A. S. O. In *Stimulation of Enzyme Activity by Oxovanadium Complexes*; Sigel, H., Sigel, A., Eds.; Metal Ions in Biological Systems, Vol. 31; Marcel Dekker: New York, 1995; Chapter 8, pp 249−285.

(10) (a) Zimmet, P.; Alberti, K. G. M. M.; Shaw, J. *Nature* **2001**, *414*, 782–787. (b) Brownlee, M. *Nature* **2001**, *414*, 813–820. (c) Moller, D. E. *Nature* **2001**, *414*, 821–827.

(11) (a) Sakurai, H.; Kojima, Y.; Yoshikawa, Y.; Kawabe, K.; Yasui, H. *Coord. Chem. Rev.* **2002**, *226*, 187–198. (b) Sasagawa, T.; Yoshikawa, Y.; Kawabe, K.; Sakurai, H.; Kojima, Y. *J. Inorg. Biochem.* **2002**, *88*, 108–112. (c) Kanamori, K.; Nishida, K.; Miyata, N.; Okamoto, K.; Miyoshi, Y.; Tamura, A.; Sakurai, H. *J. Inorg. Biochem.* **2001**, *86*, 649–656. (d) Takino, T.; Yasui, H.; Yoshitake, A.; Hamajima, Y.; Matsushita, R.; Takada, J.; Sakurai, H. *J. Biol. Inorg. Chem.* **2001**, *6*, 133–142. (e) Melchior, M.; Rettig, S. J.; Liboiron, B. D.; Thompson, K. H.; Yuen, V. G.; McNeill, J. H.; Orvig, C. *Inorg. Chem.* **2001**, *40*, 4686–4690. (f) Sun, Q.; Sekar, N.; Goldwaser, I.; Gershonov, E.; Fridkin, M.; Shechter, Y. *Am. J. Physiol. Endocrinol. Metab.* **2000**, *279*, E403–E410. (g) Goldwaser, I.; Gefel, D.; Gershonov, E.; Fridkin, M.; Shechter, Y. *J. Inorg. Biochem.* **2000**, *80*, 21–25. (h) Woo, L. C.; Yuen, V. G.; Thompson, K. H.; McNeill, J. H.; Orvig, C. *J. Inorg. Biochem.* **1999**, *76*, 251–257. (i) Brand, R. M.; Hamel, F. G. *Int. J. Pharm.* **1999**, *183*, 117–123. (j) Yuen, V. G.; Caravan, P.; Gelmini, L.; Glover, N.; McNeill, J. H.; Setyawati, I. A.; Zhou, Y.; Orvig, C. *J. Inorg. Biochem.* **1997**, *68*, 109–116.

(12) (a) Crans, D. C. In *Vanadium and its Role in Life*; Sigel, H., Sigel, A., Eds.; Metal Ions in Biological Systems, Vol. 31; Marcel Dekker: New York, 1995; Chapter 5, pp 147−209. (b) Martin, R. B. *J. Inorg. Biochem.* **1986**, *28*, 181–187.

(13) Gorzsás, A.; Getty, K.; Andersson, I.; Pettersson, L *Dalton Trans.* **2004**, *18*, 2873–2882.

(14) Kaliva, M.; Raptopoulou, C. P.; Terzis, A.; Salifoglou, A. *Inorg. Chem.* **2004**, *43*, 2895–2905.

(15) Tsaramyrsi, M.; Kavousanaki, D.; Raptopoulou, C. P.; Terzis, A.; Salifoglou, A. *Inorg. Chim. Acta* **2001**, *320*, 47–59.

(16) Kaliva, M.; Kyriakakis, E.; Gabriel, C.; Raptopoulou, C. P.; Terzis, A.; Tuchagues, J.-P.; Salifoglou, A. *Inorg. Chim. Acta* **2006**, *359*, 4535–4548.

(17) Kaliva, M.; Gabriel, C.; Raptopoulou, C. P.; Terzis, A.; Salifoglou, A. *Inorg. Chim. Acta* **2008**, *361*, 2631–2640.

(18) (a) Kiss, T.; Buglyo, P.; Sanna, D.; Micera, G.; Decock, P.; Dewaele, D. *Inorg. Chim. Acta* **1995**, *239*, 145–153. (b) Crans, D. C.; Ehde, P. M.; Shin, P. K.; Pettersson, L. *J. Am. Chem. Soc.* **1991**, *113*, 3728–3736. (c) Crans, D. C.; Felty, R. A.; Miller, M. M. *J. Am. Chem. Soc.* **1991**, *113*, 265–269. (d) Tracey, A. L.; Li, H.; Gresser, M. J. *Inorg. Chem.* **1990**, *29*, 2267–2271.

(19) (a) Fritzsche, M.; Elvingson, K.; Rehder, D.; Pettersson, L. *Acta Chem. Scand.* **1997**, *51*, 483–491. (b) Gorzsás, A.; Getty, K.; Andersson, I.; Pettersson, L *Dalton Trans.* **2003**, *12*, 2503–2511. (c) Caldeira, M. M; Ramos, M. L.; Oliveira, N. C.; Gil, S. V. M. *Can. J. Chem.* **1987**, *65*, 2434–2440.

(20) (a) Wright, D. W.; Humiston, P. A.; Orme-Johnson, W. H.; Davis, W. M. *Inorg. Chem.* **1995**, *34*, 4194–4197. (b) Zhou, Z.-H.; Wan, H.-L.; Tsai, K.-R. *Chin. Sci. Bull.* **1995**, *40*, 749. (c) Velayutham, M.; Varghese, B.; Subramanian, S. *Inorg. Chem.* **1998**, *37*, 1336–1340.

(21) Tsaramyrsi, M.; Kaliva, M.; Giannadaki, T.; Raptopoulou, C. P.; Tangoulis, V.; Terzis, A.; Giapintzakis, J.; Salifoglou, A. *Inorg. Chem.* **2001**, *40*, 5772–5779.

(22) Zhou, Z.-H.; Wan, H.-L.; Hu, S.-Z.; Tsai, K.-R. *Inorg. Chim. Acta* **1995**, *237*, 193–197.

(23) Burojevic, S.; Shweky, I.; Bino, A.; Summers, D. A.; Thompson, R. C. *Inorg. Chim. Acta* **1996**, *251*, 75–79.

(24) Skibsted, J.; Nielsen, N. C.; Bildsøe, H.; Jakobsen, H. J. *J. Am. Chem. Soc.* **1993**, *115*, 7351–7362.

(25) Sheldrick, G. M SHELXS-97: Structure Solving Program; University of Göttingen, Göttingen, Germany, 1997.

(26) Sheldrick, G. M SHELXL-97: Structure Refinement Program; University of Göttingen, Göttingen, Germany, 1997.

(27) Kaliva, M.; Giannadaki, T.; Raptopoulou, C. P.; Terzis, A.; Salifoglou, A. *Inorg. Chem.* **2002**, *41*, 3850–3858.

(28) Kaliva, M.; Raptopoulou, C. P.; Terzis, A.; Salifoglou, A. *J. Inorg. Biochem.* **2003**, *93*, 161–173.

(29) Djordjevic, C.; Lee, M.; Sinn, E. *Inorg. Chem.* **1989**, *28*, 719–723.

(30) (a) Kaliva, M.; Giannadaki, T.; Raptopoulou, C. P.; Tangoulis, V.; Terzis, A.; Salifoglou, A. *Inorg. Chem.* **2001**, *40*, 3711–3718.

(b) Gabriel, C.; Venetis, J.; Kaliva, M.; Raptopoulou, C. P.; Terzis, A.; Drouza, C.; Meier, B.; Voyiatzis, G.; Potamitis, C.; Salifoglou, A. *J. Inorg. Biochem.* **2009**, *103*, 503–516.

(31) Biagioli, M.; Strinna-Erre, L.; Micera, G.; Panzanelli, A.; Zema, M. *Inorg. Chim. Acta* **2000**, *310*, 1–9.

(32) Hambley, T. W.; Judd, R. J.; Lay, P. A. *Inorg. Chem.* **1992**, *31*, 343–345.

(33) Bourne, S. A.; Cruywagen, J. J.; Kleinhorst, A. *Acta Crystallogr, Sect. C: Cryst. Struct. Commun.* **1999**, *C55*, 2002–2004.

(34) (a) Lever, A. B. P.; Gray, H. B. *Inorg. Chem.* **1980**, *19*, 1823–1824. (b) Lever, A. B. P.; Gray, H. B. *Acc. Chem. Res.* **1978**, *11*, 348–355.

(35) Evans, D. F. *J. Chem. Soc.* **1957**, 4013–4018.

(36) Deacon, G. B.; Philips, R. *J. Coord. Chem. Rev.* **1980**, *33*, 227–250.

(37) Griffith, W. P.; Wickins, T. D. *J. Chem. Soc. A* **1968**, 397–400.

(38) Vuletic, N.; Djordjevic, C. *J. Chem. Soc., Dalton Trans.* **1973**, 1137–1141.

(39) (a) Matzapetakis, M.; Raptopoulou, C. P.; Terzis, A.; Lakatos, A; Kiss, T.; Salifoglou, A. *Inorg. Chem.* **1999**, *38*, 618–619. (b) Matzapetakis, M.; Raptopoulou, C. P.; Tsohos, A.; Papaefthymiou, B.; Moon, N.; Salifoglou, A. *J. Am. Chem. Soc.* **1998**, *120*, 13266–13267. (c) Matzapetakis, M.; Dakanali, M.; Raptopoulou, C. P.; Tangoulis, V.; Terzis, A.; Moon, N.; Giapintzakis, J.; Salifoglou, A. *J. Biol. Inorg. Chem.* **2000**, *5*, 469–474. (d) Matzapetakis, M.; Karligiano, N.; Bino, A.; Dakanali, M.; Raptopoulou, C. P.; Tangoulis, V.; Terzis, A.; Giapintzakis, J.; Salifoglou, A. *Inorg. Chem.* **2000**, *39*, 4044–4051. (e) Matzapetakis, M.; Kourgiantakis, M.; Dakanali, M.; Raptopoulou, C. P.; Terzis, A.; Lakatos, A; Kiss, T.; Banyai, I.; Iordanidis, L.; Mavromoustakos, T.; Salifoglou, A. *Inorg. Chem.* **2001**, *40*, 1734–1744.

(40) Schwendt, P.; Volka, K.; Suchánek, M. *Spectrochim. Acta* **1988**, *44A*, 839–844.

(41) Campbell, N. J.; Dengel, A. C.; Griffith, W. P. *Polyhedron* **1989**, *8*, 1379–1386.

(42) Schwendt, P.; Ahmed, M.; Marek, J. *Inorg. Chem. Commun.* **2004**, *7*, 631–633.

(43) Mimoun, H.; Saussine, L.; Daire, E.; Postel, M.; Fischer, J.; Weiss, R. *J. Am. Chem. Soc.* **1983**, *105*, 3101–3110.

(44) Baran, E. J. *J. Coord. Chem.* **2004**, *54*, 215–238.

(45) Parajon-Costa, B. S.; Piro, O. E.; Pis-Diez, R.; Castellano, E. E.; Gonzalez-Baro, A. C. *Polyhedron* **2006**, *25*, 2920–2928.

(46) Georgiadou, I.; Papadopoulou, Ch.; Matralis, H. K.; Voyiatzis, G. A.; Lycourghiotis, A.; Kordulis, Ch. *J. Phys. Chem. B* **1998**, *102*, 8459–8468.

(47) (a) Lapina, O. B.; Khabibulin, D. F.; Shubin, A. A.; Terskikh, V. V. *Prog. Nucl. Magn. Reson. Spectrosc.* **2008**, *53*, 128–191. (b) Nielsen, U. A.; Jakobsen, H. J.; Skibsted, J. *Inorg. Chem.* **2000**, *39*, 2135–2145.

(48) (a) Hagen, H.; Bezemer, C.; Boersma, J.; Kooijman, H.; Lutz, M.; Spek, A. L.; van Koten, G. *Inorg. Chem.* **2000**, *39*, 3970–3977. (b) Rehder, D. In *Studies in Inorganic Chemistry 13: Transition Metal NMR*; Pregosin, P. S., Ed.; Elsevier: Amsterdam, 1991.

(49) Ooms, K. J.; Bolte, S. E.; Baruah, B.; Choudhary, M. A.; Crans, D. C.; Polenova, T. *Dalton Trans.* **2009**, 3262–3269.

(50) Massiot, D.; Fayon, F.; Capron, M.; King, I.; Le Calvé, S.; Alonso, B.; Durand, J.-O.; Bujoli, B.; Gan, Z.; Hoatson, G. *Magn. Reson. Chem.* **2002**, *40*, 70–76.

(51) Bak, M.; Rasmussen, J. T.; Nielsen, N. C. *J. Magn. Reson.* **2000**, *147*, 296–330.

(52) Ferrer, E. G.; Baran, E. J. *Biol. Trace Elem. Res.* **2001**, *83*, 111–119.

(53) (a) Fritzsche, M.; Elvingson, K.; Rehder, D.; Pettersson, L. *Acta Chem. Scand.* **1997**, *51*, 483–491. (b) Ehde, P. M.; Andersson, I.; Pettersson, L. *Acta Chem. Scand.* **1991**, *45*, 998–1005. (c) Ehde, P. M.; Andersson, I.; Pettersson, L. *Acta Chem. Scand.* **1989**, *43*, 136–143. (d) Caldeira, M. M; Ramos, M. L.; Oliveira, N. C.; Gil, S. V. M. *Can. J. Chem.* **1987**, *65*, 2434–2440. (e) Preuss, F.; Rosenhahn, L. J. *Inorg. Nucl. Chem.* **1972**, *34*, 1691–1703.

(54) Rehder, D.; Pessoa, J. C.; Geraldes, C. F. G. C.; Margarida, M.; Castro, C. A.; Kabanos, T.; Kiss, T.; Meier, B.; Micera, G.; Pettersson, L.; Rangel, M.; Salifoglou, A.; Turel, I.; Wang, D. *J. Biol. Inorg. Chem.* **2002**, *7*, 384–396.